An assessment of relationships between the Australian subtropical ridge, rainfall variability and high-latitude circulation patterns.

Dr Allyson A.J. Williams[1]* and Dr Roger C. Stone[2]

1. *Queensland Climate Change Centre of Excellence, Nambour, Queensland, 4560, Australia.*
2. *Australian Centre for Sustainable Catchments, University of Southern Queensland, Toowoomba, Queensland, 4350, Australia.*

*Corresponding Author

Abstract

The monthly anomaly of the latitude of the subtropical ridge over eastern Australia (L) is a major regulator of synoptic-scale influences on Australia's climate. Three datasets have been used to calculate L (observed Australia coastal MSLP, Hadley and NCEP Reanalysis datasets). The choice of data sets used in this study appeared to strongly influence results. Changes in the Southern Hemisphere Hadley Cell and meridional circulation changes are associated with changes in L and it is shown that (1) L has statistically and physically significant relationships with seasonal rainfall in Australia, (2) the Antarctic Oscillation Index (AOI) has statistically significant relationships with Australian seasonal rainfall, and (3) L and the AOI and Southern Annular Mode (SAM) are significantly related. Longer-term latitudinal shifts in L are also discussed.

1. Introduction

It is recognised that the El Niño Southern Oscillation (ENSO) is the prime driver of variations in rainfall, temperature (McBride and Nicholls 1983; Stone *et al.,* 1996; Nicholls 2000; Simmonds and Hope 1997) and, especially, agronomic systems over most regions of Australia (Meinke and Hammer 1997). However, the need to identify, and if possible quantify, relationships between other climatic phenomena, rainfall, and subsequent agronomic variability in Australia remains if a greater understanding of climate systems by users and also user uptake in terms of improved managements systems that included climate information is to be enhanced and facilitated.

Pittock (1971) showed that the interannual variability of the latitude of the surface subtropical high pressure maximum over eastern Australia is a major mechanism influencing inter-annual rainfall variability, albeit less significant than the Southern Oscillation. More than 50% of the total variance in annual Australian rainfall could be accounted for by the variability in both the latitude of the subtropical ridge (STR) and in the Southern Oscillation (Pittock 1975,Trenberth 1975). The influence of the latitude of the STR is especially significant in southern Queensland and Tasmania (as shown to be statistically significant by Drosdowsky, 1993). The annual latitude of the STR also relates to the interannual variability of annual mean maximum temperatures (Coughlan 1979), zonal westerly winds (Thresher 2002), meridional wind and mean air temperature, and ozone (Pittock 1973). Seasonal relationships have been demonstrated to exist between the seasonal latitude of the STR and snow depth (Budin 1985), zonal westerly winds (Thresher 2002), and coastal heavy rain events (Hopkins and Holland 1997). These relationships have been shown to be both physically and statistically significant. Such relationships suggest that monthly anomalies of the latitude of the STR (henceforth, monthly anomalies are referred to as "L") are a proxy for the monthly climatology of mid-latitude and some subtropical synoptic-scale features.

Finally, Thresher (2002) suggested seasonally-averaged L and solar activity are related (but not statistically significant). The caveats in Thresher's data as elucidated by Drosdowsky (2005) that are so pertinent for long-term trend analyses, have only minimal effect on these relationships. Importantly, Thresher (2002) also reinforced the need to analyse synoptic shifts in L on a seasonal basis rather on an annually-averaged basis (remarkably, a point overlooked in many analyses of this type) if application of this improved knowledge is to be attained.

In addition to variability due to ENSO and the STR, the Antarctic Oscillation (AO), also referred to as the Southern Annular Mode (SAM), derived from the first EOF of anomalous southern hemisphere sub-tropical sea level pressure/height/temperature (Kidson 1988, Karoly 1990, Thompson and Wallace 2000) is also an important contributor to rainfall variability in Australia (Meneghini *et al.* 2007; Hendon *et al.* (2007).

It is surprising relatively few advances have been made in further elucidating and quantifying relationships between the STR, the SAM, and seasonal rainfall in Australia despite the fact that they appear to be major contributors to rainfall variability and may also provide improved skill for seasonal climate forecast systems.

The aim of this paper is to reassess linkages between the STR and rainfall variability in Australia using recent and longer rainfall time-series, and to quantify linkages between the STR and rainfall variability with global-scale systems such as the Southern Annular Mode.

2. Data

Monthly L anomalies were calculated from mean sea level pressure (MSLP) data recorded at the Commonwealth Bureau of Meteorology (CBoM) weather stations between 1959 and 2004, the details of which are shown in Figure 1. Monthly average MSLP data were obtained by taking the mean of monthly 9am MSLP and 3pm MSLP data. Following the basic methodology of Das (1956) and Pittock (1973) a cubic spline is applied between all stations and L is defined as the latitude at which the highest monthly MSLP was recorded. Monthly anomalies were determined using a mean monthly L value from the base period 1961-1990 and are used to remove the seasonal cycle (this time-series is called ObsL). A positive value of L means that the STR is anomalously equatorward and a negative value anomalously poleward. We recognise that measuring L at a specific longitude is not necessarily representative of any global average position of the STR or its position at any other longitude and hence the longitude of measurement should be taken into account in interpretations. However, we believe it is important to recognise and identify the most appropriate manifestation of a global-scale system such as 'the sub-tropical ridge' if relationships with rainfall and other synoptic features are to be appropriately determined (also P. McIntosh, personal communication). We emphasise we chose coastal MSLP data largely in order to capture the important contribution of coastal and near-coastal ridging along the east coast of Australia associated with the strength of the surface anticyclone commonly located in the Tasman Sea. Indeed we suggest analyses of this system requires some attention be given to synoptic features rather than simple analysis of broad scale data sets that may mask their important attributes (P. McIntosh pers. Comm., J. Butler pers. comm.).

We also created a monthly L time-series from the UK Met Office Hadley Centre's MSLP data set, HadSLP2 (Allan and Ansell 2006), and a daily and monthly L from the National Centres for Environmental Prediction-National Centre for Atmospheric Research (NCEP/NCAR) reanalysis data set (Kalnay *et al.*, 1996). As shown by Drosdowsky (2005) there are many ways to calculate an L index. To enable better comparison of different studies (eg Pittock 1973, Drosdowky 2005, Thresher 2002), we use the area-averaging technique and splining suggested by Drosdowsky (2005) to calculate L from the NCEP and Hadley gridded MSLP datasets. That is, to calculate the NCEP daily (NCEPDL) and monthly (NCEPL) L we use L values calculated from MSLP averaged across longitudes 147.5E, 150.0E and 152.5E that has had a cubic-spline applied across the latitudes 0-65^{o}S (as per Drosdowky 2005). NCEPDL was calculated each day from daily MSLP and then averaged to create a monthly L mean. NCEPL was calculated from monthly MSLP. Both indices extend from 1948 to 2002.

The above area-averaging and splining techniques were also applied to the monthly HadSLP2 data, except the longitudinal averaging of was across 145-150-155^{o}E. The HadSLP2 dataset is a combination of monthly fields of pressure observations on a 5-degree latitude-longitude grid from 1850 to 2004. The resultant monthly L index is called HadL.

The gridded MSLP data on a 2.5-degree grid from the NCEP/NCAR reanalysis data were also used to calculate monthly L values (as per above) at all longitudes on the grid, that is, at every 2.5 degrees of longitude. These other approximations of L are collectively called $NCEPL_{longitudes}$ and will be used to show larger-scale relationships between circulation indices and the position of the STR at longitudes other than the Australian eastern coast. The same process is used with the HadSLP2 dataset to calculate monthly L values at gridpoints at every 5 degrees of latitudes ($HadL_{longitudes}$).

As Drosdowsky (2005) states, a cubic-spline between the stations/gridpoints creates a "continuous variable" as opposed to a "categorical" variable across the latitudes, and we have used it here to enable easier comparison between studies. However, the effect it has on the L time-series is minimal and we suggest it is not critical for future studies. The R^2 between monthly anomalies of L-not-splined and the L-splined using the observed datasets was approximately 0.95 for all three L time-series (ObsL, HadL, NCEPL).

Vertical motion (omega) and temperature at 17 levels throughout the atmosphere was also obtained from the NCEP/NCAR reanalysis data. Caution must be observed when using the NCEP reanalysis data in the data-sparse latitudes of the Southern Ocean however, as there are biases (Marshall, 2003), although this mainly applies to analyses of trend and less so to variability.

A 0.25 degree grid of monthly rainfall from 1890 to 2004 was obtained from the National Climate Centre, Australia (Jones and Weymouth 1997).

The Southern Oscillation Index (SOI), the Antarctic Oscillation Index (AOI), the Quasi-biennial Oscillation (QBO), and the Decadal Solar Oscillation (DSO) were also used for analytical purposes. The AOI reflects the oscillation of large-scale anomalous SLP between the mid and high latitudes (eg Kidson 1988,Thompson and Wallace 2000). The Antarctic Oscillation (AO) is also referred to as the Southern Annular Mode (SAM) and is the first EOF of anomalous southern hemisphere sub-tropical sea level pressure/height/temperature (Kidson 1988, Karoly 1990, Thompson and Wallace 2000). In addition to the first EOF of SLP there are approximately three commonly used indices of the SAM. Gong and Wang (1999) calculate the AOI (AOI-GW) as the difference between normalized zonally-averaged SLP at 40^{o}S and 65^{o}S from NCEP/NCAR reanalysis data: when the SLP at 40^{o}S is high the SLP around 60-70^{o}S is low, and vice versa. We have used Marshall's (Marshall 2003) AOI (AOI-Marshall) which is different to the NCEP/NCAR Reanalysis-derived AOI of Gong and Wang (1999) and the EOF-derived SAM Index of Thompson and Wallace (2000), known as AOI-EOF. Marshall's version of this index which uses the mean MSLP observations from six stations located approximately at each of the two latitudes to provide a proxy zonal mean. The benefit of the Marshall index is that it

avoids the bias in the NCEP/NCAR reanalysis data in the high latitudes of the Southern Hemisphere (eg Randel and Wu 1999, Marshall 2002, 2003).

Monthly SOI values were supplied by the Queensland Department of Primary Industries and Fisheries. This SOI was initially developed by Troup (1965) and defined as the difference in MSLP anomalies between Tahiti and Darwin (where the base period for the mean is from 1887 to 1989), divided by the standard deviation of the differences, and multiplied by ten.

As previous investigations had identified potential for relationships between the latitude of the STR and solar activity (e.g. Kidson 1925; Thresher 2002), monthly solar data were also obtained from the online catalogue of the sunspot index generated by R.A.M. Van der Linden and SIDC at http://sidc.oma.be/html/sunspot.html.

The Quasi-Biennial Oscillation (QBO) is also an important contributor to southern hemisphere rainfall variability (Jury et al., 1994; 2004) and so relevant data and methods related to the QBO were included in this study. The stratospheric QBO (a stratospheric zonal wind change between east and west with an average, although highly variable, periodicity around 28 months) (see Baldwin *et al.* 2001 for a review) has also been found to significantly modulate the effect of solar variability on stratospheric and tropospheric circulation (eg Labitzke 2004). The QBO data are monthly means of the zonal wind component measured at Canton Island, 3°S/172°W (Jan 1953 - Aug 1967), Gan/Maledive Islands, 1°S/73°E (Sep 1967 - Dec 1975) and Singapore, 1°N/104°E (since Jan 1976) (Labitzke and collaborators 2002). Following Labitzke (2004) we stratify our data into years when the QBO was westerly (positive) and easterly (negative). However, although Labitzke used the 45hPa QBO, we found the strongest apparent relationships between rainfall and solar activity were associated with the QBO at 70hPa.

3. Results

3.1 The importance of defining an L index.

The aim of this section is to emphasize the importance of the influence of how L is defined and also the choice of dataset used to create the index. This section also builds on the work of Drosdowsky 2005. The time-series of the monthly values of the de-seasonalized four L indices are shown in Figure 2. The time-series of annual averages (January-December mean) of each L index are shown in Figure 3. The ObsL is generally further north than the other three indices by approximately two degrees of latitude. This is a reflection of a coastal index that captures the coastal ridging along the east coast of Australia.

Although Pearson's correlation coefficient indicates the time-series of four indices are all significantly correlated to each other (as shown in Table 1), there are important differences between the indices in terms of long term trends (Table 1, Figure 3, and Figure 4) and the annual cycle (Figure 5). The correlations show that the difference between the NCEPDL and NCEPL is less than that between NCEP and HadL and ObsL. It has been documented in previous studies that the annual mean of daily STR is more poleward than the annual mean of monthly STR (Drosdowsky 2005, Jones and Simmonds 1994), but that they have similar interannual variation (Drosdowsky 2005).

The literature also presents different accounts (Drosdowsky 2005, Thresher 2003) of the annual cycle of L, which we show here to be dependent on the dataset and precise measurement methodology. Figure 5 shows the seasonal cycle of ObsL is furthest south in March and north in August. Both the HadL and NCEPL have a maximum in August, but their minimum occurs in February. NCEPDL also has a minimum in February but a maximum in September. The NCEPDL cycle is the same as in Drosdowsky (2005) but the monthly L indice maximums are different.

Differences persist in regard to opinion on the level of variability of the STR over the past 50 years. (Drosdowsky 2005, Thresher 2003). Partitioning all four L dataset into two epochs, 1959-1975 and 1976-2002, suggests differing apparent trends evident according to the particular selection of each of the four indices (Figure 6). All four indices have a February minimum in the earlier epoch, and only NCEPDL and ObsL change in the later epoch to a minimum occurring in March.

The occurrence of the winter most northerly position varies more between datasets than the summer minimum. In the early epoch the maximum occurs in July (NCEPL), August (ObsL and HadL), and September (NCEPDL). In the later epoch both the HadL and ObsL have not changed from a maximum in August but the NCEPL and NCEPDL occur in September. Interestingly, although HadL is the only index to show a significant trend in annual average values of L (Figure 3), the annual cycle doesn't change from a February minimum and August maximum.

As well as changes in the months of seasonal extremes, all four indices show a change in the shape of the seasonal cycle from the earlier epoch where the index drops in June to the later epoch where the index rises steadily from May through August/September (Figure 6). (difficult figure to understand, I think)…maybe we can present it in a different way?

3.2 Relationships between variability of L and rainfall.

Correlations between ObsL and seasonal rainfall are shown in Figure 7. Negative correlations between ObsL and rainfall mean that when L is anomalously poleward, anomalously high seasonal rainfall is

likely in the areas depicted. Positive correlations mean that when L is anomalously poleward, rainfall is relatively low. These linear relationships indicate that the amount of year-to-year variability in seasonal rainfall that is accounted for by variations in L ranges from approximately 60% in winter in Tasmania and Victoria, to around 30% in early summer in New South Wales.

The four L indices (ObsL, HadL, NCEPL, NCEPDL) have very similar spatial patterns of correlations with rainfall when compared over their common time frame 1959-2002. However there are differences and these may or may not be relevant depending on the purpose of the analysis. For example if the scale of relevance is 1000kms then the differences may not be noted, however if the scale of relevance is less than 100kms or for a particular rainfall-catchment for example, then the differences will be important. As an example of this, the L-rainfall correlations for December-January-February and June-July-August for all four indices are shown in Figure 9. In the December-February season all four indices have significant negative correlations in the eastern region of the country and significant negative correlations in south-western Tasmania. The overall pattern of correlations is very similar between the four indices, however differences include (a) the boundary between positive and negative correlations in the southern mainland area which is further south in both the NCEPL and NCEPDL maps; (b) HadL has a smaller area of negative correlations along the eastern sea-board; and (c) a different pattern in the south-west of Australia, to name but a few. In the July-August season all four indices have significant positive correlations in Victoria, Tasmania, and significant negative correlations in the far eastern coast of Australia. The main differences are that (a) HadL and NCEPL have greater expanses of negative correlations in inland and north-west Australia than ObsL and NCEPDL; (b) the significant positive ObsL correlations in the south-west cover a greater area than for the other indices (NCEPDL has no significant correlations in this area); and (c) all except NCEPDL have significant negative correlations in the north east.

The relationship between L and SAM (AOI-Marshall) is discussed and shown in Table 2: when SAM is positive, L is poleward. Interestingly the AOI-rainfall relationships for the same period (Figure 8) indicate that spring rainfall, as shown by predominantly positive Sep-Nov correlations with SAM, is higher when SAM is in a positive mode. The correlations between rainfall and both indices prove to be coherent.

The apparent relationships between SAM and Australian rainfall appear to be similar to those between L and rainfall and various aspects in relation to SAM/rainfall relationships have recently been discussed by Meneghini *et al.* (2007) and Hendon *et al*. (2007). As indicated in Figure 8, there are strong relationships (statistically significant) for many seasons, and a certain consistency in the relationships between seasons indicating potentially high physical significance. Spring and summer seasons are dominated by positive correlations between SAM and rainfall over Western Australia and NSW/QLD, indicating that when the AOI is positive there is an increase in rainfall in those regions.

The negative correlations between SAM and rainfall in autumn and winter in the southern regions of southwest Western Australia, Victoria, and Tasmania, indicate that when the AOI is negative there is an increase in rainfall in those regions.

As mentioned in the earlier Section 2 discussing data, there are at least three indices of SAM: an EOF-derived AOI, the Gong and Wang AOI, and the Marshall AOI. There has been discussion in the literature (eg Marshall 2002, 2003) regarding the differences in the various indices and the effect of different datasets used to calculate them. The different indices also have different relationships with Australian rainfall as shown in Figure 10. For example, correlations between seasonal rainfall and the Gong and Wang AOI as in Meneghini *et al.* (2007) are different to the correlations shown here that use the Marshall AOI. We call for caution when comparing results of SAM studies that use different indices. The seasonal relationships between June-July-August rainfall and each of the AOIs, and also for December-January-February is shown in Figure 10. The correlations in the June-August period are consistent in the western half of the continent: all three indices have significant positive correlations with rainfall. However there are large differences in the eastern half of the continent with the GW (Figure 10(a)) and Marshall (Figure 10(b)) AOIs having significant positive correlations with rainfall yet the EOF AOI have negative correlations (not statistically significant). The December-February relationships are similar for the three indices in the south-west of Australia (Figure 10 (d)-(e)-(f)), but different elsewhere. The most marked difference is between the AOI-GW (Figue 10(d)) where there are significant positive correlations in eastern Australia, and the AOI-EOF (Figure 10(f)) which has negative correlations up the east coast and not statistically significant negative correlations further inland.

3.3 Relationship between L and circulation patterns at high and low latitudes.

Previous studies relating the variability of L to various modes of atmospheric variability suggest that L may be influenced by both high-latitude circulation patterns (eg Thresher 2002) and equatorial variability (eg Pittock 1984). Drosdowsky (2005) reports that L and the SOI are significantly correlated (r=+0.33) however this is at the annual timescale with no mention of seasonal relationships. It is suggested annual data are not appropriate in this instance as relationships may be seasonal and, as shown in Table 2, seasonal L is not related to the SOI, except slightly so in summer (also pointed out by Lough 1991). The negative correlations between ObsL and the AOI-Marshall shown in Table 2 are significant throughout most of the year but are stronger between May and September. The negative correlation indicates that when the AOI is negative, L is positive, that is: the latitude of the STR is further south.

Figure 11 shows the correlations between AOI and both the monthly HadL and NCEPL. As in Sections 3.1 and 3.2, the importance of datasets is shown to be important as there are large differences between the correlations between $HadL_{longitudes}$ and AOI, and $NCEPL_{longitudes}$ and AOI mainly in the Indian Ocean (50^oE-100^oE).

There are statistically significant correlations between both $HadL_{longitudes}$ and $NCEPL_{longitudes}$ and the AOI across much of the Southern Hemisphere although the correlations are weak over the eastern Pacific Ocean (approx longitude 130^oW) and South America (70^oW). This region is also the region where the SAM signal is weakest in the EOF loadings shown in Figure 1 of Thompson and Wallace (2000). The significant negative correlations between monthly $HadL_{longitudes}$/$NCEPL_{longitudes}$ and the AOI suggest that when the AOI is positive (that is there is a positive SLP anomaly at 40^oS greater than that at 65^oS) the subtropical highs are not only stronger and the subpolar lows deeper (as in Gong and Wang 1999) but $HadL_{longitudes}$/$NCEPL_{longitudes}$ is also further south. These weak correlations are statistically significant at the 95% level but, as with many such relationships (such as those between SOI and rainfall shown by Simmonds and Hope 1997), are not stationary over time (data not shown). These weak but significant relationships between the SAM and LSTR are in keeping with the potential of the SAM to affect and be affected by circulation and climate at latitudes outside the polar regions (eg Gong and Wang 1998, Thompson and Wallace 2000).

Hall and Visbeck (2002) show that in the region 20^oS-45^oS a positive AOI correlates with easterly wind anomalies indicating a poleward shift of the midlatitude jetstream, and also increased subsidence between 35^oS-55^oS. Assuming L is related to the position of the midlatitude jetstream, the negative correlation between ObsL and AOI-Marshall means that when the AOI is positive, the jetstream is poleward concurring with the results in Figure 7.

These meridional interactions imply changes should also be seen in meridional circulations such as the Hadley and Ferrel Cells as STR moves anomalously equatorward and poleward. The meridional influences of ObsL on the meridional temperature gradients are shown in Figure 12 and the vertical motion omega in Figure 13. As shown in Figure 12, when comparing the zonally averaged temperatures of the composites of years when ObsL is anomalously north and the years when ObsL is anomalously south, there is mostly a positive difference in the seasonal means south of approximately 50^oS in the austral winter and spring. This means that when STR is anomalously equatorward, the hemispheric meridional temperature gradient decreases as temperatures at higher latitudes increase and those at lower latitudes decrease. The effect is strongest in Aug-Oct and is strongest in the stratosphere. Although only data for the seasonal averages Jun-Aug, Jul-Sep, and Aug-Oct are shown, the effect continues through to early summer (Nov-Jan). The decreased temperature gradient is indicative of greater poleward transport of heat and hence a stronger Hadley Cell (Hou 1998).

A stronger Hadley Cell when STR is equatorward can also be seen in the vertical velocity data. Figure 13(d) shows the average seasonal (Jul-Sep) distribution of zonally-averaged omega (positive omega is downward motion): in the austral winter the ITCZ is north of the equator; the downward arm of the Hadley Cell is between 30-10^{o}S; and there is a distinct upward arm at 60^{o}S. Each of the 3-monthly seasons Figure 13(a) Figure 13(b) Figure 13(c), have a similar pattern of omega anomalies: in the downward arm of the Hadley Cell (between 10 and 30^{o}S) omega increases in years when ObsL is anomalously equatorward. That is, there is greater downward motion (not statistically significant). To the north of this there is a slight decrease in omega (statistically significant in Jul-Sep and Aug-Oct), indicating the strength of uplift increases. At the polar region (80^{o}S), there is also an increase in omega, indicating stronger downward motion. Although the data aren't as clear as the temperature gradients, they could still reflect stronger meridional circulation. At 60^{o}S the zone of negative omega (Figure 13(d)) is less negative when ObsL is north indicating weaker uplift. Although this is suggestive of a weaker Ferrel Cell, the area of decreased omega anomalies north of that region (around 40^{o}S) could indicate a shift north of the cell.

The observed AOI/SAM also displays a trend towards the positive mode (although not statistically significant), whereas the NCEP/NCAR reanalysis data displays a highly statistically significant trend towards the positive mode, although this may be due to biases in the data network of the Southern Ocean. The use of the observed data may reconcile an issue raised by Drosdowsky (2005). For example Drosdowsky (2005) shows no trend in the latitude of STR, as opposed to Thresher (2002, 2003). In addition, unlike the EOF-based indices, the observed data can more readily be updated.

Timescales of coherent variability

Co-spectral analysis is used to assess the timescales on which seasonal STR and SAM have greatest coherency. The dominant timescales of variability of monthly ObsL are shown in the spectral plots of Figure 14. The data were detrended to achieve stationarity, tapered (15%), and padded to a power of 2. Spectral density estimates were obtained from the periodograms using Hamming weights with a moving average window of width of 5. The presence of cycles in the monthly ObsL time-series was tested using Bartlett's Kolmogorov-Smirnov d-statistic; the test showed that although there were physically significant peaks in the periodogram, there was statistically little difference from white noise. In order to strengthen the spectral signal, we utilised three different smoothed monthly ObsL time-series: a 3-month running mean of monthly ObsL, a 12-month running mean, and also used a January-December mean of ObsL. The resultant Bartlett Kolmogorov-Smirnov d-statistics for the individual periodograms of these smoothed time-series were all statistically significant. We use all four time-series of ObsL (that is, monthly, 3-monthly means, 12-monthly means, and an annual mean) in the spectral analyses shown in Figure 14 and 15 as firstly it shows the effect of different data manipulations, and secondly it increases the robustness of patterns of variability if the same patterns are found in each time-series.

As shown in Figure 14, monthly ObsL has significant modes of variability at 146 months, 36-38 months, 26-28 months, 22-24 months, 9-10 months and 5 months. The timescales at which SAM is most related to STR are shown in the plots of a cross-spectral analysis of ObsL and AOI-Marshall (the AOI-Marshall monthly time-series is smoothed as per the monthly ObsL) in Figure 15. As shown by the co-spectral density values the ObsL and AOI-Marshall indices are most strongly related on timescales of 24 months and 38 months. High squared coherency values indicate that 70 and 75% of the ObsL variability at these timescales is accounted for by AOI-Marshall. The phase statistic (not shown) indicates that at these two key timescales the AOI-Marshall index leads the ObsL, however the behaviour of the two indices at these relatively short periodicities is complex and because of the lack of consistency between periodicities we suggest the results should be interpreted cautiously. The 24-month cycle has a positive phase (AOI-Marshall leads by 11-12 months), but the 26-month cycle has a negative phase and 27-29 month cycle has a positive phase. The 38 month cycle has a negative phase for all three monthly time-series and flips to positive between 39-68 months (SAM leads by 18 months). However this uncertainty at 38-39 months is reduced by considering the results of the annual time-series which has a positive phase from approximately 33 months onwards (SAM leads ObsL by approximately 17 months at the 38-39 month cycle).

There are also interesting but less significant peaks at 144 months and 256 months. AOI-Marshall accounts for approximately 75% of the variability of ObsL at 144-months, but only about 20% at 256-months. All cycles longer than 100 months have a negative phase (that is, the ObsL leads AOI-Marshall). At 256 months the ObsL leads AOI-Marshall by approximately 124 months. The ObsL 144-month cycle leads AOI-Marshall cycle by 45 months.

3.4. Solar relationships with L and AOI

The wavelet analysis of Figure 16 shows that the 144-month cycle is present over the entire time-series. This 12-year spectral peak is in close agreement with both Kidson (1925) and Thresher (2002) who found an approximate 11 year cycle (ranges between 9 and 13) in the position of L over eastern Australia. There are suggestive connections to solar forcing but identifying a plausible mechanism remains a considerable challenge. Thresher (2002) implies a relationship between solar activity and the sub-tropical ridge (not statistically significant) and suggests it may be driven by expansion and contraction of the Antarctic Polar Vortex. Labitzke (2004) shows that the SAM is related to the solar cycle and the equatorial stratospheric QBO.

Seasonal correlations between solar activity and ObsL are shown in Table 3. With the exception of seasons starting in August and September, the significance of the correlation is very low. In the Aug-Oct and Sep-Nov seasons the correlation is positive (significance level is 0.12) which suggests that in

years of solar maximum, the subtropical ridge tends equatorward. These weak (but statistically significant) results are in keeping with the general finding of Thresher (2002) who found that in solar maxima in Jun-Aug L is further north. However our results do not support his conclusion that in Dec-Feb L is further south in solar maxima. This may well be due to the discrepancies in the Thresher (2002) dataset (Drosdowsky 2005). We note though that Shindell *et al*. (1999) found a poleward shift in the Northern Hemisphere subtropical jetstream in DJF during solar maximum, which agrees in principle with Thresher (2002).

The relationship between solar activity and the AOI-Marshall was also investigated as shown in Table 3. With the exception of a significance level of 0.16 in Aug-Oct and May-Jul (α =0.06), the correlations were also of low statistical significance. The results from these two seasons are in keeping with Baldwin and Dunkerton (2005) who found that solar modulation of the arctic polar vortex is greatest in the boreal winter. In these months the negative correlation indicates that in years of solar maxima, the SAM tends to be in its negative mode. Although the lack of continued statistical significance across the seasons in the correlations makes conclusions questionable, the correlation coefficients are in parallel with the general relationship between solar activity and ObsL for this season. That is, the relationship between STR and SAM as shown in Table 2 implies that in years of maximum solar activity, when the SAM is in a negative mode, STR should be further equatorward, concurring with the solar activity/STR correlations in Table 3.

The weakness of these correlations and the lack of seasonal consistency led us to follow Labitzke (2004) who found stronger relationships between solar activity and climate parameters when grouping the years according to the equatorial stratospheric QBO. Table 4 shows the same correlations as in Table 3 but when grouped according to the QBO phase. Generally, the correlations between solar activity and the AOI-Marshall are strongest in the east QBO phase compared with the west phase although marked exceptions include 3-monthly seasons starting in May, June, and September. Also, the correlations tend to be opposite in the east phase compared to the west phase. For both QBO phases, the relationships are strongest in late austral winter, spring, early summer: this includes the seasons Jul-Sep, Aug-Oct, Sep-Nov. In the east phase only, there are also significant correlations in Feb-Apr and Mar-May. In the east phase the correlations are positive in winter/spring which indicates that during solar maxima the AOI-Marshall is positive. From Table 4, the negative r values (although not statistically significant) between solar activity and ObsL indicate that ObsL is further poleward during the solar maxima/east phase by nearly 4 degrees of latitude. It is believed the use of dynamic general circulation models (GCMs) that could include possible solar activity forcing may offer the potential to further elucidate these possible relationships discussed here.

4. Discussion

The variations in the latitude of the subtropical ridge over Australia are known to modify Australian rainfall, and it is the purpose of this paper to further elucidate on these relationships.

It is clear that the method and data used to calculate indices of L and SAM must be clearly defined and results from subsequent studies using different indices of the same phenomenon compared with caution. Building on Drosdowsky (2005) we show that the time-series of ObsL, HadL, and NCEPL although significantly correlated have different characteristics that have important consequences. These divergences include differences in (1) long-term trends, (2) changes in the seasonal cycle, (3) seasonal relationships with rainfall. There are also large differences between the $HadL_{longitudes}$ and $NCEPL_{longitudes}$ correlations with AOI with the $NCEPL_{longitudes}$ correlations generally stronger, especially in the Indian Ocean region. The departure from the expected smooth seasonal cycle was noted by Pittock (1971) and may be related to changes in the semi-annual oscillation (SAO, Van Loon *et al*. 1993, Simmonds and Jones 1998). The SAO weakened in the midlatitudes in the late 1970s (Van Loon *et al.* 1993) and although a trend in the 5-month spectral peak is not evident in the wavelet analysis of Figure 16 this may be due to 3-month smoothing of the time-series. There is a break in the pattern of spectral densities around 1980 which may be relevant but requires further study to determine a cause. In addition, there has been speculation that the changes in the SAO is related to a southward trend in a zonally averaged STR between 1972 and 1989 (Van Loon *et al.* 1993). It is not known however what L-index time-series was used in that study. This study questions the notion of a southward shift in the STR over the past 50 years however, depending on the specific L time-series used there do appear to be trends in certain seasons. The southward shift of the STR in May-June-July is possibly followed by a northward shift in June-July-August.

The other significant issue regarding datasets and methodologies is the difference between the monthly mean latitude of the daily STR (NCEPDL) and the latitude of the monthly mean STR (NCEPL) (Drosdowsky 2005, Gibson 1992). A subjective assessment of those analyses that use all four time-series show that, although there are differences between NCEPDL and NCEPL, many of the differences are less or equal to that between the three time-series ObsL, HadL, and NCEPL (for example, the monthly and seasonal correlations and trends in Table 1 and Figure 4, and annual data in Figure 3).

It is evident that higher winter rainfall occurs in the southeast of Australia when the STR is anomalously poleward, in agreement with Pittock (1971) and Thresher (2002) who conclude that L reflects the position of the rain bearing easterly and westerly wind system. The relationships between SAM and Australian rainfall in spring and summer are dominated by positive correlations between SAM and rainfall over Western Australia and NSW/QLD. This increase in rainfall when the AOI is

positive may be reflecting stronger easterlies in NSW/Qld and greater convergence with the monsoon trough both of which tend to occur when the summer high pressure cells are more intense. The axis of the zonally averaged storm track closely coincides with the westerly jet axis, though only weakly in austral winter (Nakamura and Shimpo 2004).

The latitude of the high pressure belt and the latitude of the subtropical jetstream (STJ), the midlatitude jetstream (MLJ), and Hadley Cell are clearly dynamically coupled (Pittock 1973 suggests that L and the STJ are essentially different aspects of the same atmospheric phenomenon) but the precise governing processes are not fully understood (see Hou 1998). For example, the STR is often used as the definition of the boundary between the tropical and midlatitude atmospheres. As described by Lorenze and Hartman (2001) the poleward edge of the STR, characterised by the rapid horizontal temperature changes of its baroclinicity, is the MLJ which is driven by internal forces of eddies. This is in contrast to the 200mb STJ at 30^{o}S which is driven by the external force of seasonal heating, the mean latitude of which approximates that of the STR (Pittock 1973). The speed of the STJ is influenced by the strength of the Hadley Cell which then influences the baroclinicity from the subtropics to the midlatitudes, regulating the poleward heat transport between the mid and high latitudes (Hou 1998). It therefore appears that the STR is a function of both the STJ and the MLJ, the dynamics of which are dominated by rate of supply of angular momentum by the Hadley Circulation and the mean-flow deceleration by extratropical eddies, the degree of baroclinic wave activity and heat transport (in fact Feldstein and Lee 1996 discuss the dominant mode of angular momentum, which is also used as a definition of NAM/SAM, in the Northern Hemisphere which is a variation of the STJ not the MLJ).

There are a number of previous studies regarding the relationship between the SAM/Zonal Index and Southern Hemisphere circulation. North-south fluctuations of the MLJ about its mean position are essentially similar to fluctuations in the SAM (Hall and Visbeck 2002, Thompson and Wallace 2000). The observations from this study are therefore related to those that focus on the variations in SAM and latitude of the MLJ, and also STJ and Hadley Cell strength etc. In their analysis of the SAM and Southern Hemisphere circulation, Thompson and Wallace (2000) observe when the tropospheric SAM in November is in a positive mode the subtropical high is weaker and the Hadley and Ferrel Cells are located more poleward. We have shown here that this corresponds to a more poleward L (shown in Table 2 and Figure 7). As shown in Figures 12 and 13, when L is anomalously poleward there is decreased poleward transport of heat indicating a weaker Hadley Cell which is also indicative of a decrease in the poleward transport of westerly momentum and other atmospheric parameters such as ozone. The linear correlations imply that the reverse is true when L is anomalously equatorward.

5. Conclusions

We used MSLP data sets from CBoM, NCEP, and Hadley Centre to construct values of L, and NCEP/NCAR reanalysis data to investigate changes in the Hadley Cell and meridional circulation changes associated with changes in L.

The most significant results from this work are:

1. The comparison of the analyses using the observed values of L, 'Hadley Centre' reanalysis values of L, and the NCEP Reanalysis datasets demonstrates that the choice of dataset will influence those results obtained in identifying relationships between L and associated rainfall and circulation pattern variation.
2. Monthly observed values of L (ObsL) display significant modes of variability at 144 months, 36-38 months, 26-28 months, 22-24 months, 9-10 months and 5 months.
3. Wavelet analysis suggests that the 144-month cycle is present over the entire time-series. There are suggestive connections to solar forcing but identifying a plausible mechanism remains a considerable challenge that may be assisted by use of general circulation models forced by solar variability inputs.
4. L has statistically and physically significant relationships with seasonal rainfall variability in Australia. Future analysis will include assessing how much information and atmospheric mechanisms this coastal L could be 'hiding', especially coastal systems. For example, coastal ridging will increase the value of L, but east coast cyclones will decrease it. An L value that is not influenced so much by synoptics may be a better discriminator and more reliable climate analysis tool.
5. The AOI/SAM has statistically significant relationships with seasonal rainfall in Australia. The relationships between SAM and Australian rainfall in spring and summer are dominated by positive correlations between SAM and rainfall over Western Australia and NSW/QLD. This increase in rainfall when the AOI is positive may be reflecting stronger easterlies across NSW/Qld and greater convergence with the monsoon trough both of which tend to occur when the summer high pressure cells are more intense.
6. Monthly L and the AOI/SAM are significantly related, especially at 3-4 years and 2 years.
7. L and the AOI/SAM may possibly be related to solar activity, mainly in winter/spring, and more strongly when the years are separated into easterly and westerly phases of the equatorial stratospheric QBO. However, it is suggested these relationships need to be further explored using coupled ocean-atmosphere general circulation models.

In terms of the L and/or AOI having potential for climate forecasting, Thompson *et al.* (2005) show that tropospheric SAM anomalies extend to 3 months following stratospheric vortex anomalies in at least the September-December period. We suggest there is potential to apply this knowledge in

development of seasonal climate forecasting systems given the apparent strong relationship between L, the AOI/SAM, and seasonal rainfall in Australia and potentially in other similar regions worldwide.

6. References

Allan, R. J. and T. J. Ansell, 2006: A new globally complete monthly historical mean sea level pressure data set (HadSLP2): 1850-2004. *J. Climate*, **19**, 5816-5842.

Baldwin, M. P. and T. J. Dunkerton, 2005: The solar cycle and stratosphere–troposphere dynamical coupling. *J. Atmos and Solar-Terrestrial Physics*, **67,** 71-82.

Baldwin, M. P., L. J. Gray, T. J. Dunkerton, K. Hamilton, P. H. Haynes, W. J. Randel, J. R. Holton, M. J. Alexander, I. Hirota, T. Horinouchi, D. B. A. Jones, J. S. Kinnersley, C. Marquardt, K. Sato, and M. Takahashi, 2001: The Quasi-Biennial Oscillation. *Reviews of Geophysics*, **39,** 179-229.

Budin, C. R., 1985: Interannual variability of Australian Snowfall. *Australian Meteorological Magazine.*, **33,** 145-159.

Coughlan, M. J., 1979: Recent variations in annual-mean maximum temperatures over Australia. *Q. J. Roy. Met. Soc*, **105,** 707-719.

Das, S.C., 1956: Statistical analysis of Australian pressure data. *Aust. J. of Physics*,**9**, 394-399.

Drosdowsky, W., 1993: An analysis of Australian seasonal rainfall anomalies: 1950-1987. I: spatial patterns. *Int. J. Climatol.*, **13,** 1-30.

Drosdowsky, W., 2005: The Latitude of the Subtropical Ridge over Eastern Australia: The L-index Revisited. *Int. J. Climatology*, **25**, 1291-1299.

Feldstein, S. and S. Lee, 1996: Mechanisms of Zonal Index Variability in an Aquaplanet GCM. *J. Atmos. Sci.*, **53**, 3541–3556.

Gong, D. Y. and S. W. Wang, 1999: Definition of Antarctic Oscillation Index. *Geophysical Research Letters*, **26,** 459-462.

Gong, D. Y. and S. W. Wang, 1998: Antarctic oscillation: concept and applications. *Chinese Science Bulletin*, **43**, 734-738.

Hall, A. and M. Visbeck, 2002: Synchronous variability in the southern hemisphere atmosphere, sea ice, and ocean resulting from the annular mode. *J. Climate*, 15 (21), 3043-3057.

Hendon, H.H., D.W.J. Thompson, and M.C. Wheeler, 2007: Australian rainfall and surface temperature variations associated with the Southern Annular Mode. *J. Climate.*,**20**, 2452-2467.

Hopkins, L. C. and G. J. Holland, 1997: Australian heavy-rain days and associated east coast cyclones: 1958-92. *J. Climate*, **10**, 621-635.

Hou, A. Y., 1998: Hadley Circulation as a Modulator of the Extratropical Climate. *J. of the Atmospheric Sciences.*, **55**, 2437-2457.

Jones, D.A. and I. Simmonds, 1994: A climatology of Southern Hemisphere anticyclones, *Climate Dynamics*, **10** (6-7), 333-348.

Jones, D. A. and G. Weymouth, 1997: An Australian monthly rainfall dataset. *Technical Report No. 70, Bureau of Meteorology.* Melbourne. 19pp.

Jury, M.R., McQueen, C., and K. Levey, 1994: SOI and QBO signals in the African region. *Theoretical and Applied Climatology*, **50** (1-2), 103-115.

Jury, M.R., W.B. White, and C.R. Reason, 2004: Modelling the dominant climate signals around southern Africa. *Climate Dynamics*, **23**, 7-8, 717-726.

Kalnay, E., M. Kanamitsu, R. Kistler, W. Collins, D. Deaven, L. Gandin, M. Iredell, S. Saha, G. White, J. Woollen, Y. Zhu, A. Leetmaa, and B. Reynolds, M. Chelliah, W. Ebisuzaki, W. Higgins, J. Janowiak, K.C. Mo, C. Ropelewski, J. Wang, Jenne, R., and Joseph, D., 1996: The NCEP/NCAR 40-Year Reanalysis Project. *Bull. of the Amer. Meteor. Soc.*, **77,** 437–472.

Karoly, D. J., 1990: The role of transient eddies in low-frequency zonal variations of the Southern Hemisphere circulation. *Tellus*, **42A,** 41-50.

Kidson, E., 1925: Some periods in Australian Weather, Bulletin No 17, 25pp pp.

Kidson, J. W., 1988: Indices of the Southern Hemisphere Zonal Wind. *J. Climate*, **1,** 183-194.

Labitzke, K., 2004: On the signal of the 11-year sunspot cycle in the stratosphere over the Antarctic and its modulation by the Quasi-Biennial Oscillation (QBO). *Meteorologische Zeitschrift*, **13,** 263-270.

Labitzke, K. and collaborators, 2002: *The Berlin Stratospheric Data Series. – CD from Meteor. Institute, Free University Berlin.*

Limpasuvan, V. and D. L. Hartmann, 1999: Eddies and the Annular Modes of Climate Variability. *Geophys. Res. Lett.*, **26,** 3133-3136.

Lorenz, D.J., and D.L. Hartmann, 2001: Eddy–Zonal Flow Feedback in the Southern Hemisphere. *J. Atmos. Sci.*, **58**, 3312–3327.

Lough, J. M., 1991: Rainfall variations in Queensland, Australia: 1891-1986. *Int. J. Climatology*, **11,** 745-768.

Marshall, G. J., 2002: Trends in Antarctic Geopotential Height and Temperature: A comparison between Radiosonde and NCEP–NCAR Reanalysis Data. *J. Climate*, **15,** 659-674.

——, 2003: Trends in the southern annular mode from observations and reanalyses. *J. Climate*, **16,** 4134-4143.

McBride, J. L. and N. Nicholls, 1983: Seasonal relationships between Australian rainfall and the Southern Oscillation. *Mon. Wea. Rev.*. **111,** pp 1998-2003.

Meinke, H. and G. L. Hammer, 1997: Forecasting regional crop production using SOI phases: an example for the Australian peanut industry. *Aust. J. Agric. Res.*, **48,** pp 789-793.

Meneghini, B., I. Simmonds, I. N. Smith, 2007: Association between Australian rainfall and the Southern Annular Mode, *Int. J. Climatology*, **27 (1),** 109-121.

Nakamura, H., and A. Shimpo, 2004: Seasonal Variations in the Southern Hemisphere Storm Tracks and Jet Streams as Revealed in a Reanalysis Dataset. *J. Climate*, **17**, 1828–1844.

Nicholls, N., 2000: El Nino/Southern Oscillation: aftermath of the 1997/1998 event and prediction of future events. *World Meteorological Organisation Bulletin*, **49,** 267 - 270.

Pittock, A.B., 1971: Rainfall and the general circulation. *Int. Conference in Weather Modification. Canberra.* "International Conference in Weather Modification." Canberra, September 6-11, 1971. p330-338. AMS, 373pp.

——, 1973: Global Meridional interactions in stratosphere and troposphere. *Q. J. Roy. Met.*

——, 1975: Climatic Change and the Patterns of variation in Australian Rainfall. *Search*, **6,** 498-504.

——, 1980: Patterns of climatic variation in Argentina and Chile. *Mon. Wea. Rev.*, **108,** 1347-1361.

——, 1984: On the reality , stability, and usefulness of southern hemisphere teleconnections. *Australian Meteorological Magazine*, **32,** 75-82.

Randel, W. J. and F. Wu, 1999: Cooling of the Arctic and Antarctic polar stratospheres due to ozone depletion. *J. Climate*, **12,** 1467–1479.

Shindell, D., D. Rind, N. Balachandran, J. Lean, and J. Lonergan, 1999: Solar variability, ozone, and climate. *Science*, **284,** 305-308.

Simmonds, I. and P. Hope, 1997: Persistence characteristics of Australian rainfall anomalies. *Int. J. Climatol.*, **17**, 597-613.

Simmonds, I., and D. A. Jones, 1998: The mean structure and temporal variability of the semiannual oscillation in the southern extratropics. *Int. J. Climatol.*, **18,** 473-504.

Stone, R. C., N. Nicholls, and H. G. L., 1996: Frost in Northeast Australia: Trends and Influence of the Southern Oscillation. *J. Climate*, **9,** 1896-1909.

Thompson, D. W. and J. M. Wallace, 2000: Annular modes in the extratropical circulation. Part 1: month-to-month variability. *J. Climate*, **13,** 1000-1016.

Thompson, D. W. J., M. P. Baldwin, and S. Solomon, 2005: Stratosphere-troposphere coupling in the Southern Hemisphere. *J. Atmos. Sci.*, **62,** 708-715.

Thresher, R. E., 2002: Solar correlates of Southern Hemisphere mid-latitude climate variability. *Int. J. Climatology*, **22,** 901-915.

Thresher, R. E. (2003), Long-term trends in the latitude of the sub-tropical ridge over southeast Australia: Climate correlates and consequences, *Proc., 7th Southern Hemisphere Meteorological Conference,* Wellington, NZ, 24– 28 March.

Torrence, C. and G. P. Compo, 1998: A Practical Guide to Wavelet Analysis. *Bull. Amer. Meteor. Soc.*, **79,** 61-78.

Trenberth, K. E., 1975: A quasi-biennial standing wave in the Southern Hemisphere and interrelations with sea surface temperatures. *Q. J. Roy. Met. Soc.*, **101,** 55-74.

Troup, A. J., 1965: The Southern Oscillation. *Q. J. Roy. Met. Soc*, **91,** 490-506.

Van Loon, H., J.W. Kidson, and A.B. Mullan, 1993: Decadal variation of the annual cycle in the Australian Dataset. J. Climate, **6**, 1227-1231.

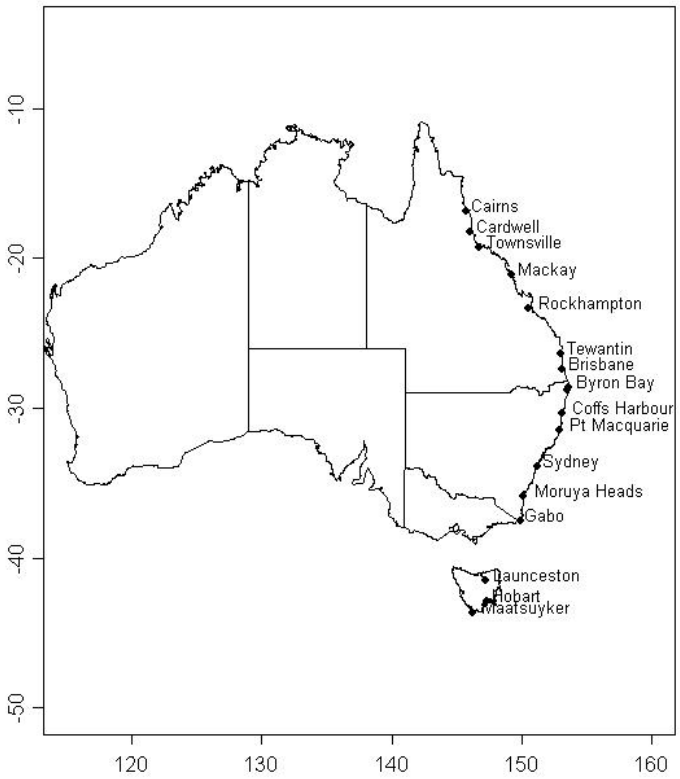

station number	name	latitude (oS)	longitude (oE)	start year	end year	missing data (%)[a]	
31011	Cairns Aero	-16.87	145.74	1941	2005	0	
32004	Cardwell Eden St	-18.25	146.02	1938	2005	0.4	
32040	Townsville Aero	-19.24	146.76	1951	2005	0	
33119	Mackay M.O	-21.11	149.21	1950	2005	2	
39083	Rockhampton Aero	-23.37	150.47	1939	2005	0	
40223	Brisbane Aero	-27.41	153.11	1951	2000	0.2	b
40842	Brisbane Aero	-27.39	153.12	2000	2005	0.2	b
58216	Byron Bay (Cape Byron Aws)	-28.63	153.63	2002	2005	0	b
58009	Byron Bay (Cape Byron Lighthouse)	-28.63	153.63	1957	2002	9	b
59040	Coffs Harbour Mo	-30.31	153.11	1951	2005	0	
60026	Port Macquarie (Bellevue Gardens)	-31.43	152.91	1909	1994	0	b
60139	Port Macquarie Airport Aws	-31.43	152.86	1995	2005	1	b
66037	Sydney Airport Amo	-33.94	151.17	1951	2005	0	
69018	Moruya Heads Pilot Station	-35.90	150.15	1957	2005	0	
84016	Gabo Island Lighthouse	-37.56	149.91	1908	2005	1	
91104	Launceston Airport Comparison	-41.54	147.20	1951	2004	1.5	
94029	Hobart (Ellerslie Road)	-42.89	147.32	1893	2005	0.2	
94041	Maatsuyker Island Lighthouse	-43.65	146.27	1945	2005	0.4	

[a]. for the period of analysis from 1959 to 2004.
[b]. these stations are appended as per recommendations from ABOM

Figure 1. The location and details of observing stations used to calculate ObsL.

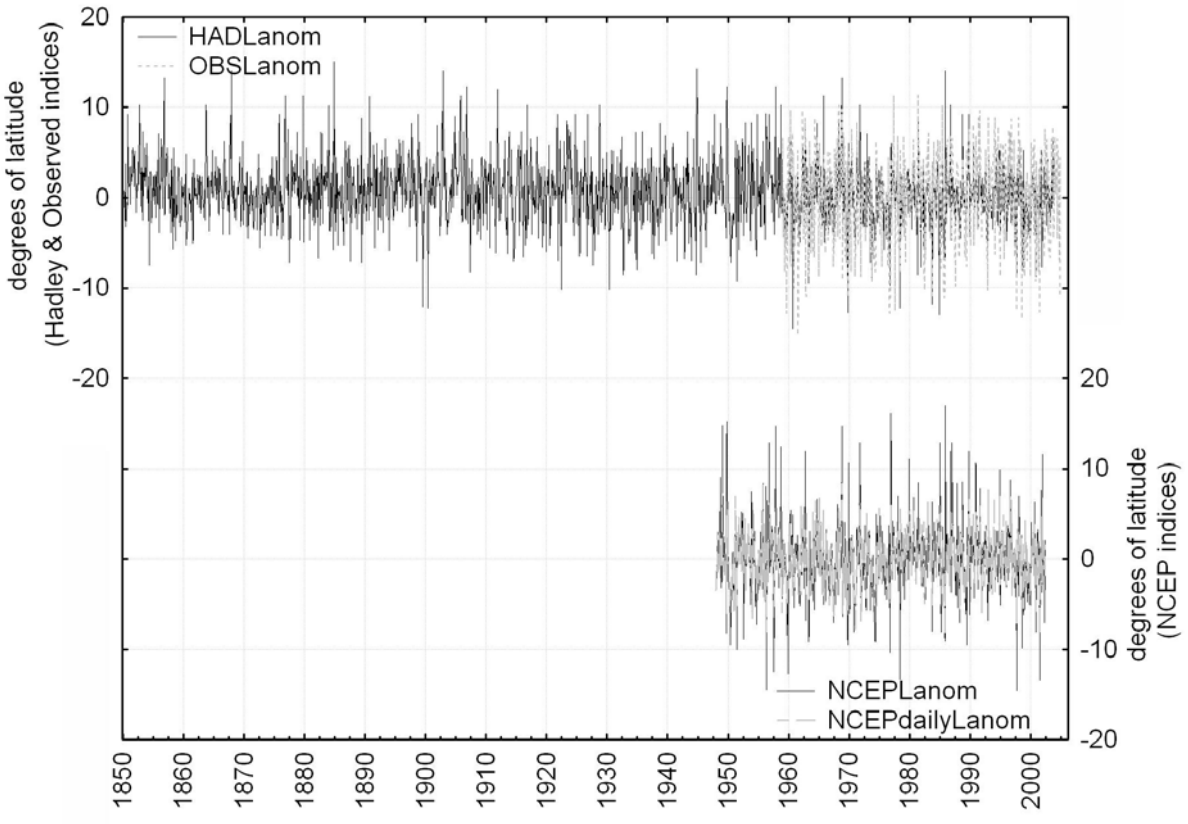

Figure 2. Time-series of monthly anomalies of the 4 L indices. To minimise clutter the HadL and ObsL are presented in the upper portion of the graph (left x-axis) and the two NCEP indices are in the lower portion of the graph (right x-axis).

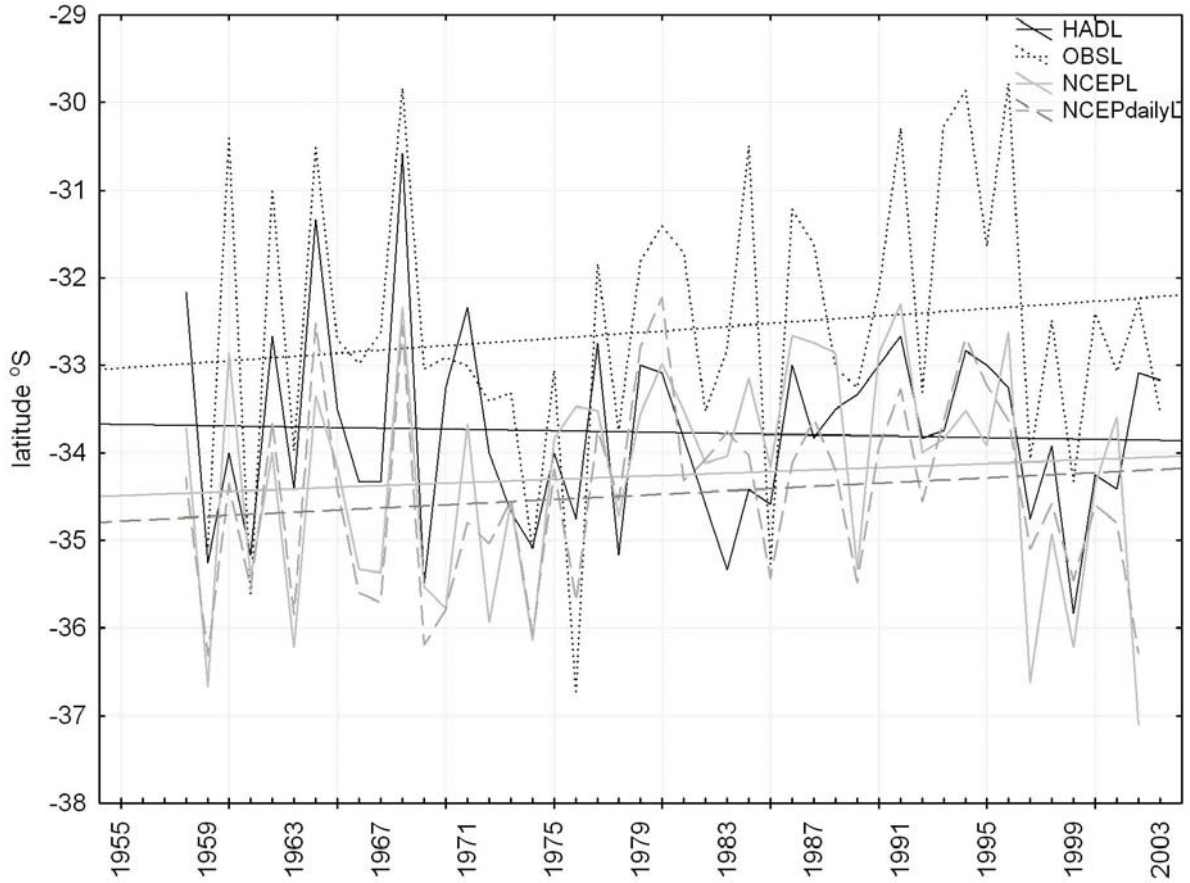

Figure 3. Time-series of January-December averaged L and a simple linear regression plot for each of the 4 L indices.

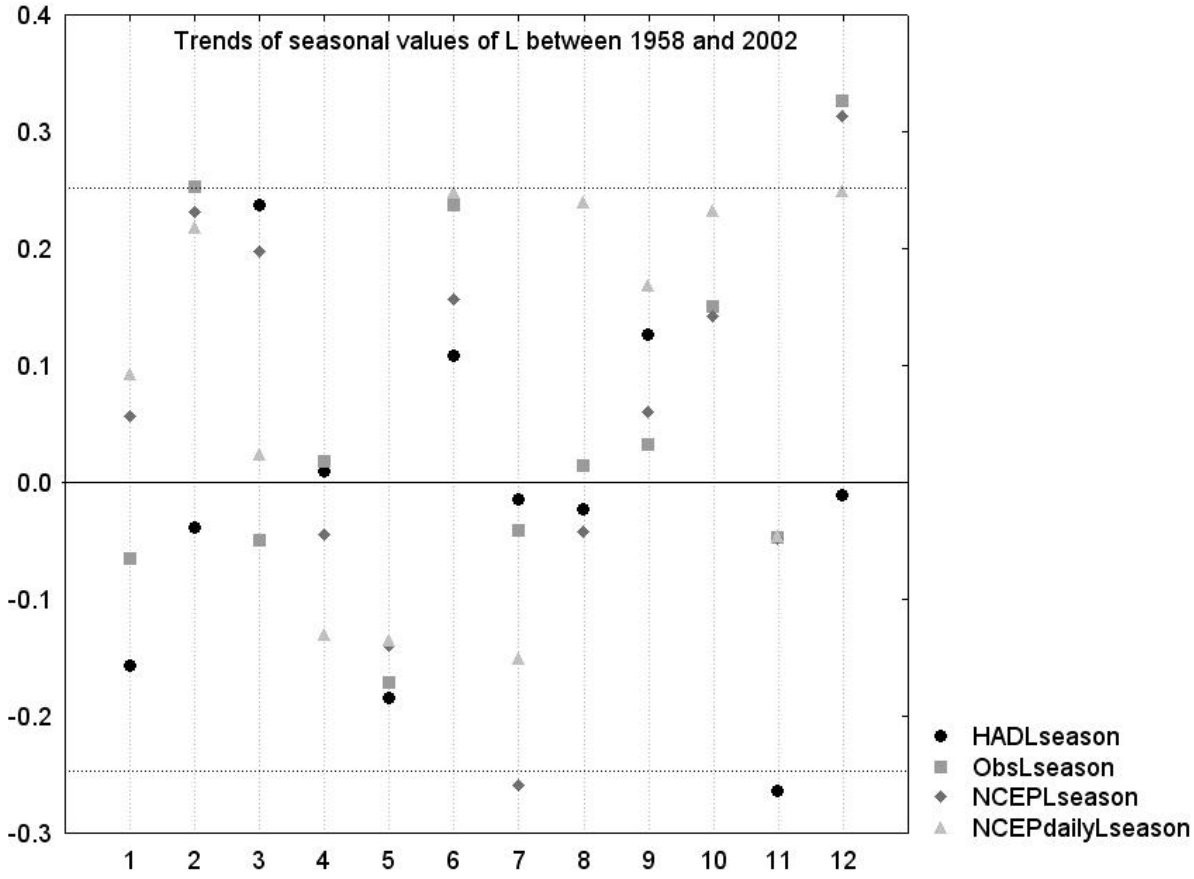

Figure 4. The trend for each season (3-monthly averaged values of L) for each of the four indices for the period 1958 to 2002. The 0.05 significant level is shown by the dotted line.

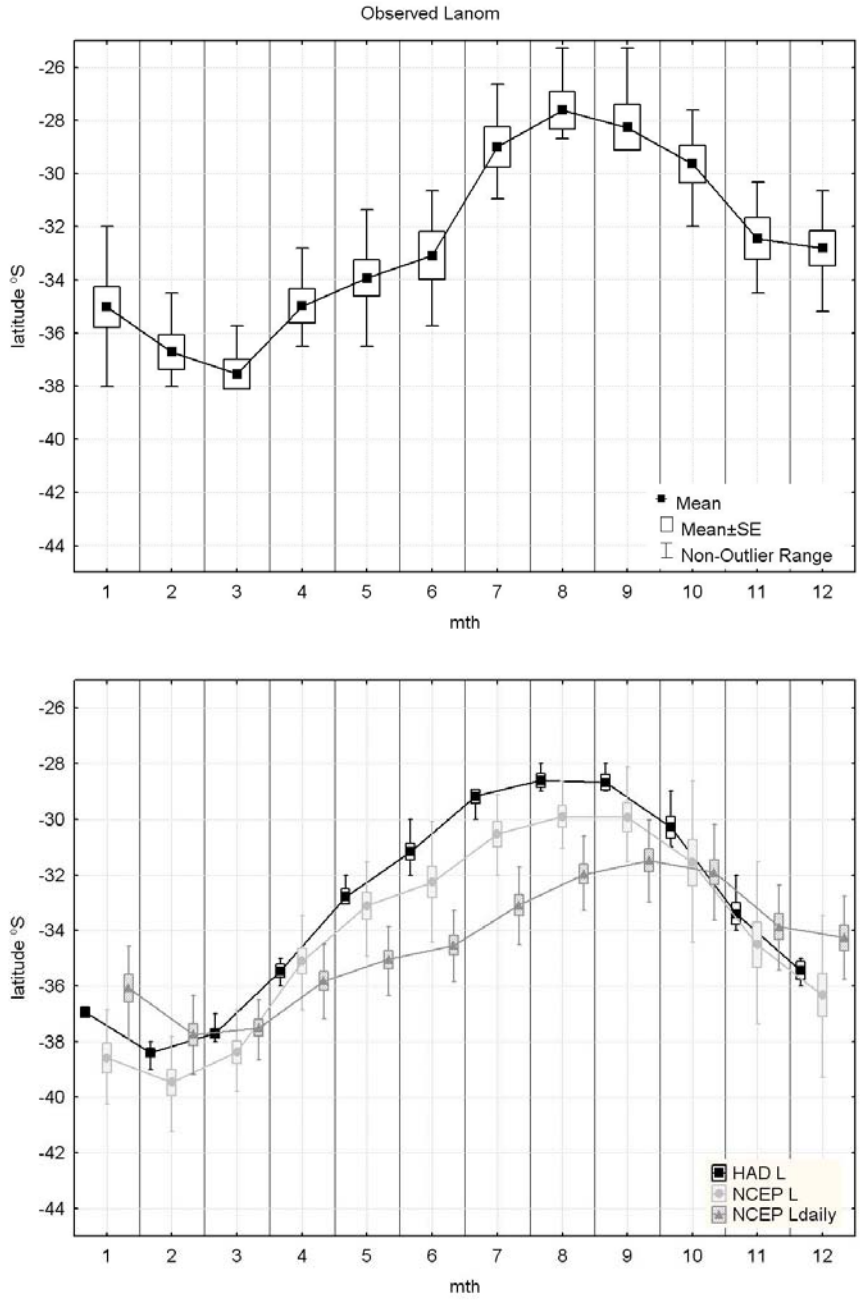

Figure 5 . The annual cycle of L for (a) the observed data and (b) the NCEP and Hadley data sets between 1958 and 2002.

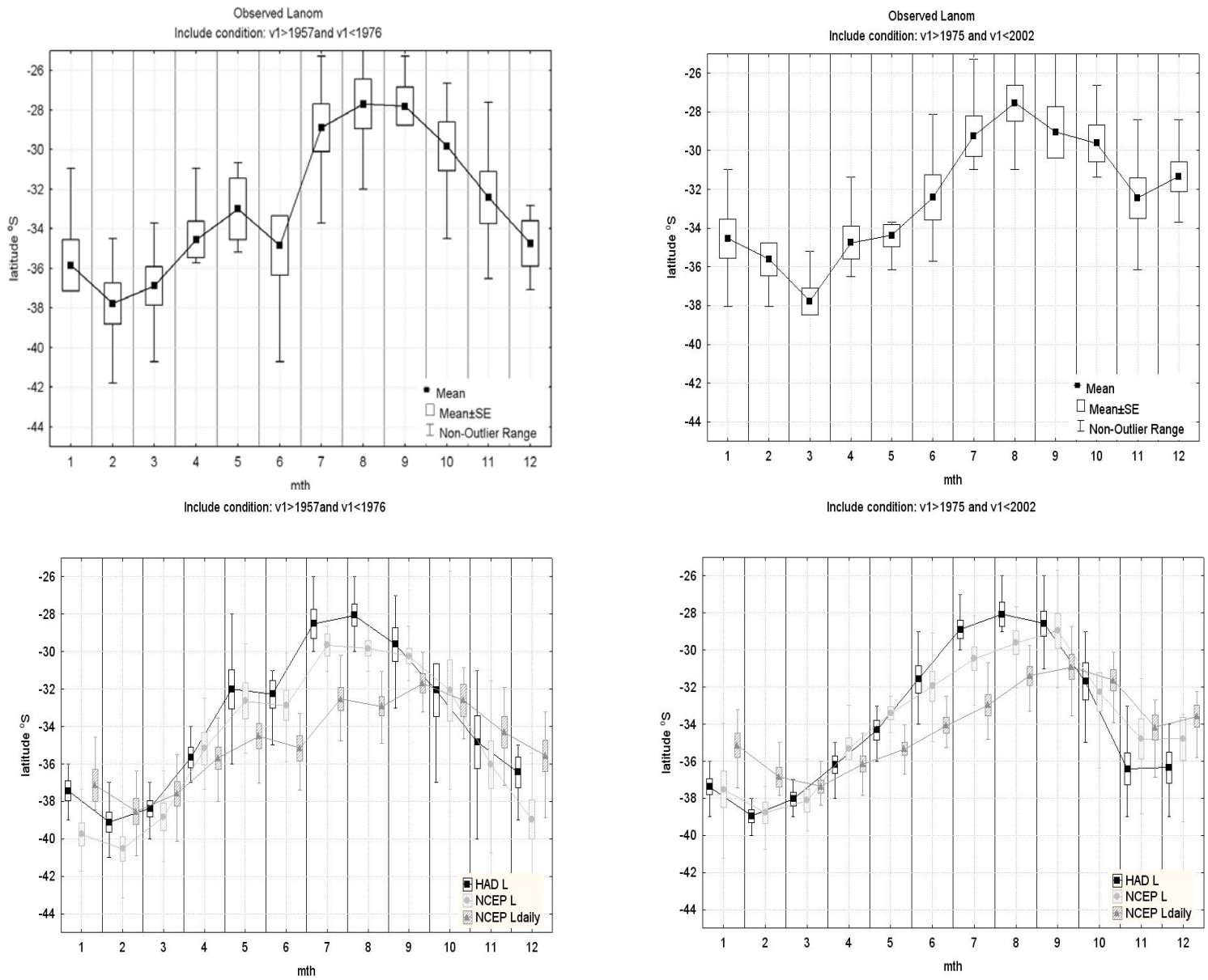

Figure 6. The change in the annual cycle in all four time-series between 1957-1975 and 1976-2002.

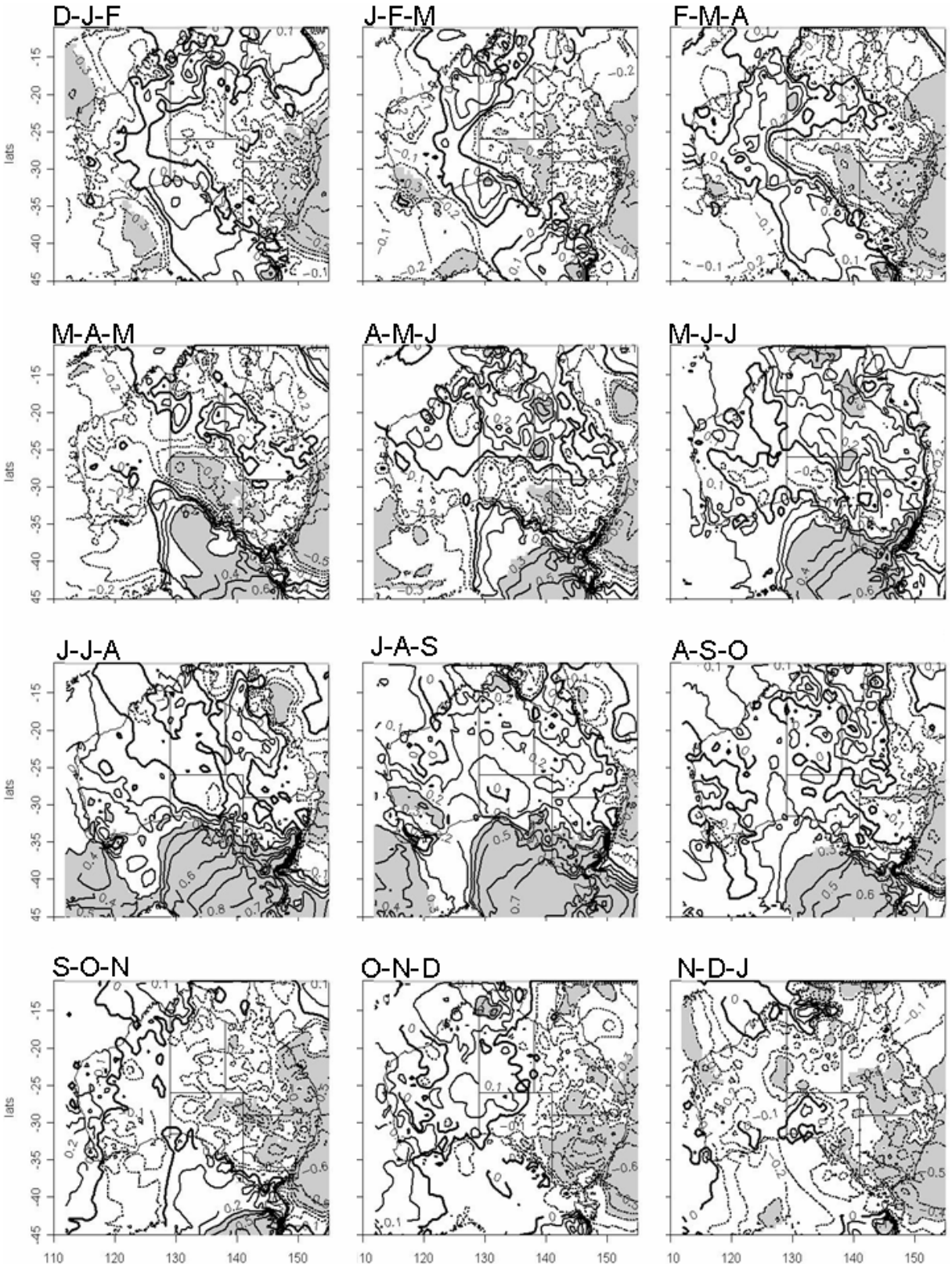

Figure 7. Pearson's correlation coefficient for seasonal values of ObsL and rainfall; negative correlations (dotted lines), positive correlations (solid line), correlations significant at the 0.05 level (shaded areas).

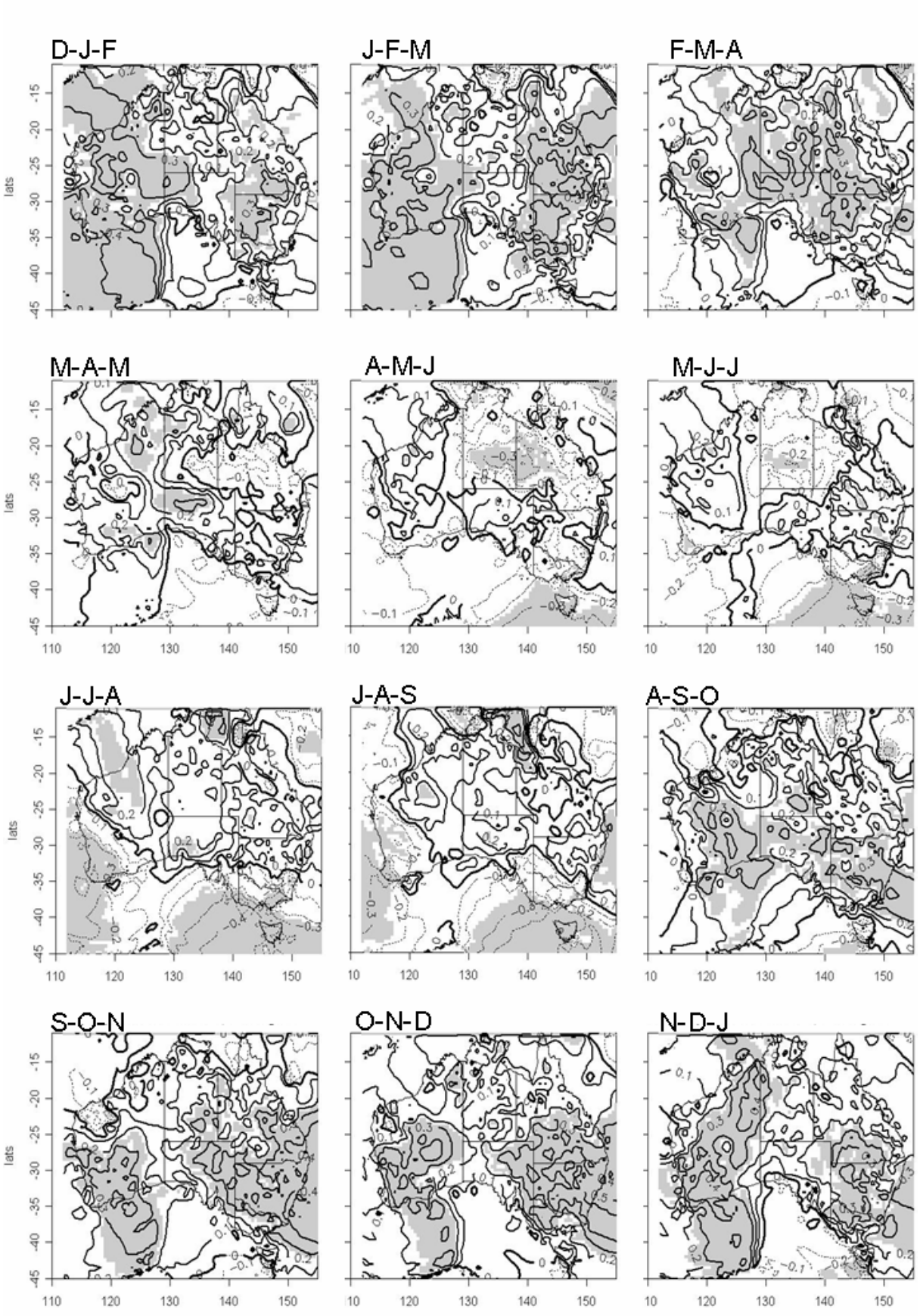

Figure 8. Pearson's correlation coefficient for seasonal values of AOI-Marshall and rainfall; negative correlations (dotted lines), positive correlations (solid line), correlations significant at the 0.05 (shaded areas).

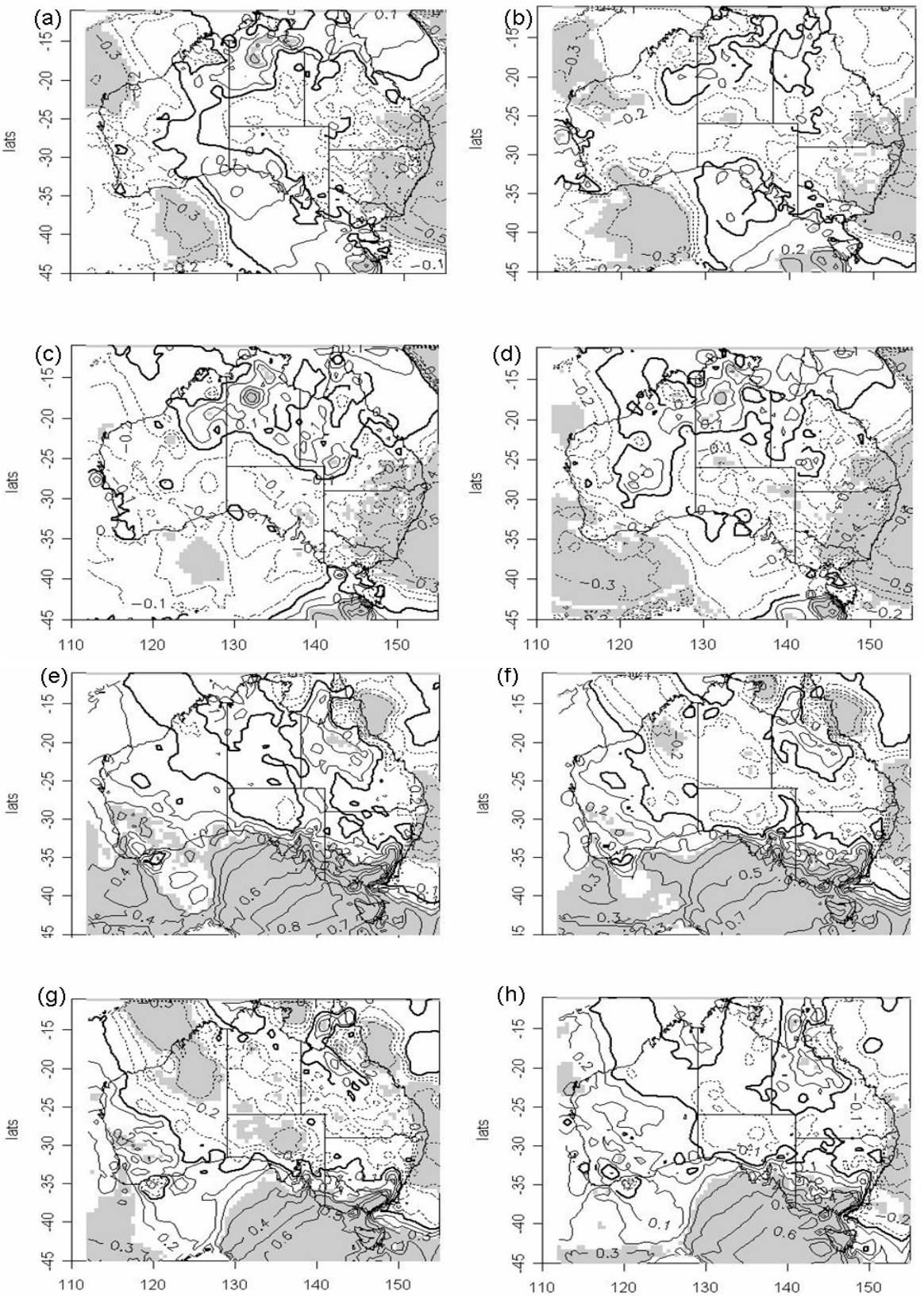

Figure 9. Pearson's correlation coefficient for December-January-February rainfall and the corresponding seasonal L value for each of the four L indices between 1959-2002 (a) ObsL (b) HadL (c) NCEPL (d) NCEPDL, and the June-July-August total rainfall and (e) ObsL (f) HadL (g) NCEPL (h) NCEPDL. Dotted Lines: negative correlations. Solid Lines: positive correlations. Shaded areas: correlations significant at the 0.05 level.

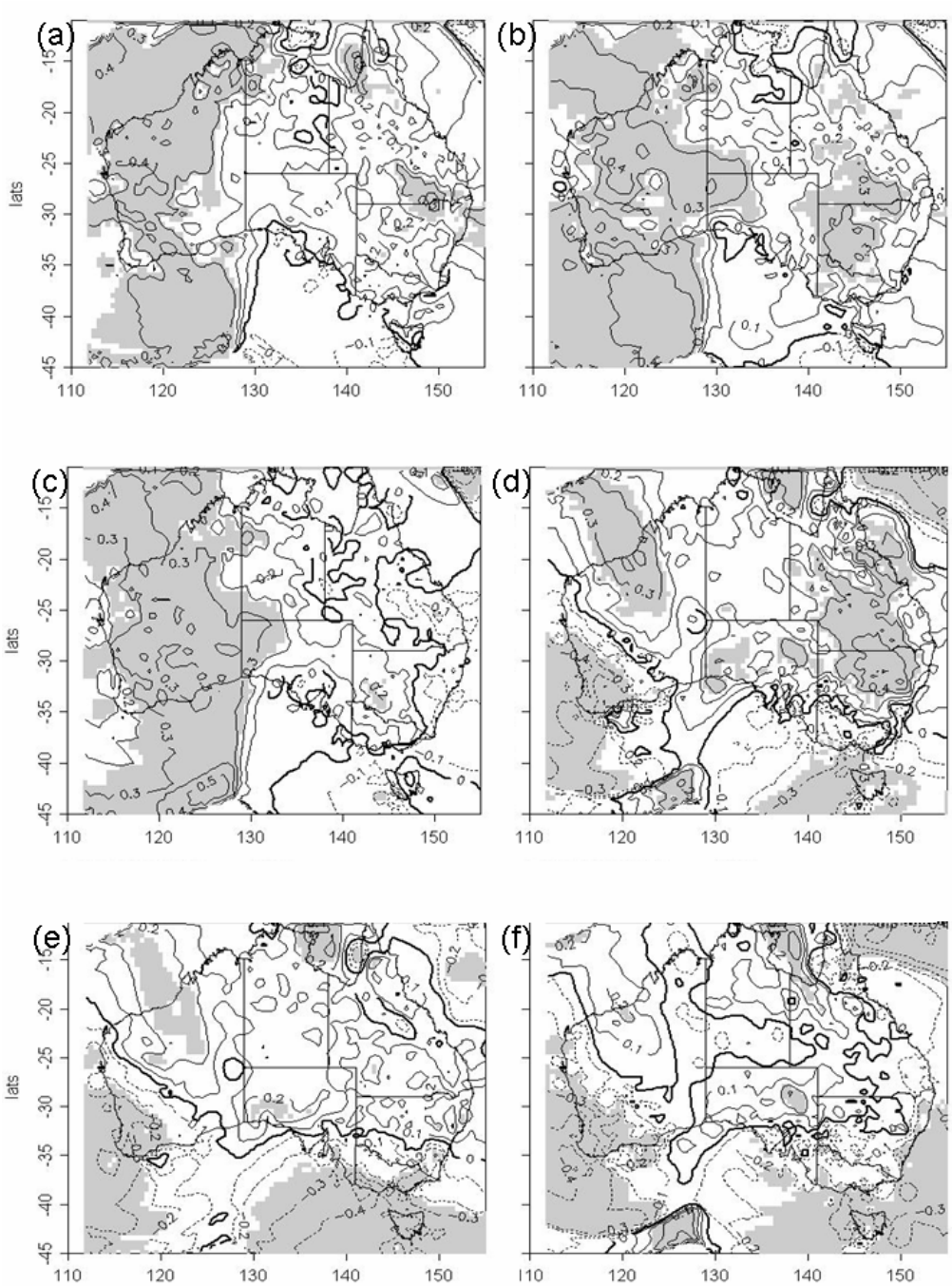

Figure 10. Comparing Pearson's correlation coefficient between seasonal rainfall and indices of SAM for December-January-February (a) AOI-GW (b) AOI-Marshall (c) AOI-EOF, and June-July-August (d) AOI-GW (e) AOI-Marshall (f) AOI-EOF.

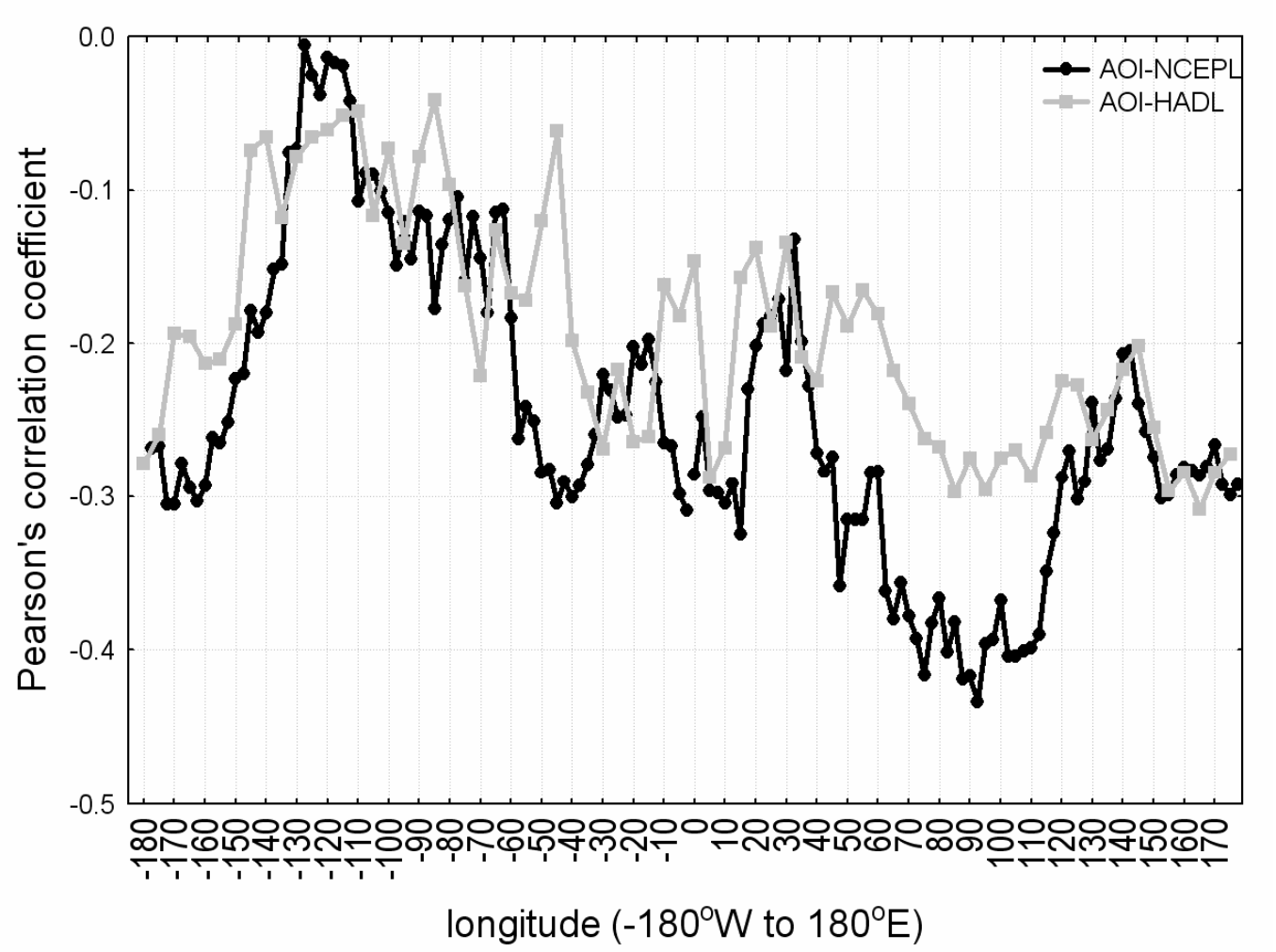

Figure 11. The Pearson correlation coefficient between the AOI-Marshall time-series and monthly NCEPL values at every 2.5 degrees of longitude (black line), and monthly HadL values at every 5 degrees of longitude. N= 504, and a correlation coefficient of 0.1 or greater is significant at 0.05 level.

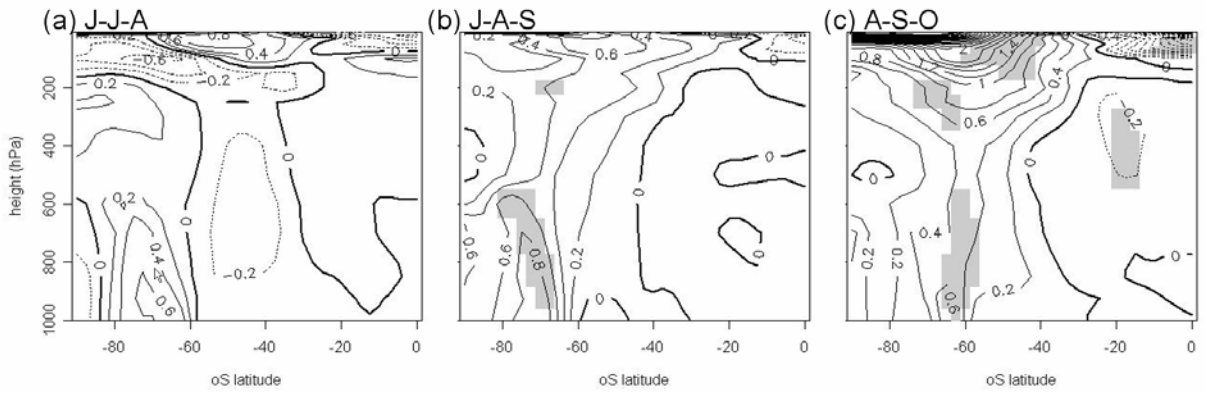

Figure 12. The zonally averaged temperature difference between averages of the composites of years of anomalously low-latitude ObsL and anomalously high-latitude ObsL for (a) June-July-August (b)July-August-Sept, (c) August-Sept-October. The solid line indicates regions of positive temperature anomalies when ObsL is in low latitudes, and the dotted line shows areas of decreased temperatures. Shaded areas are those that are significant at the 0.05 significance level.

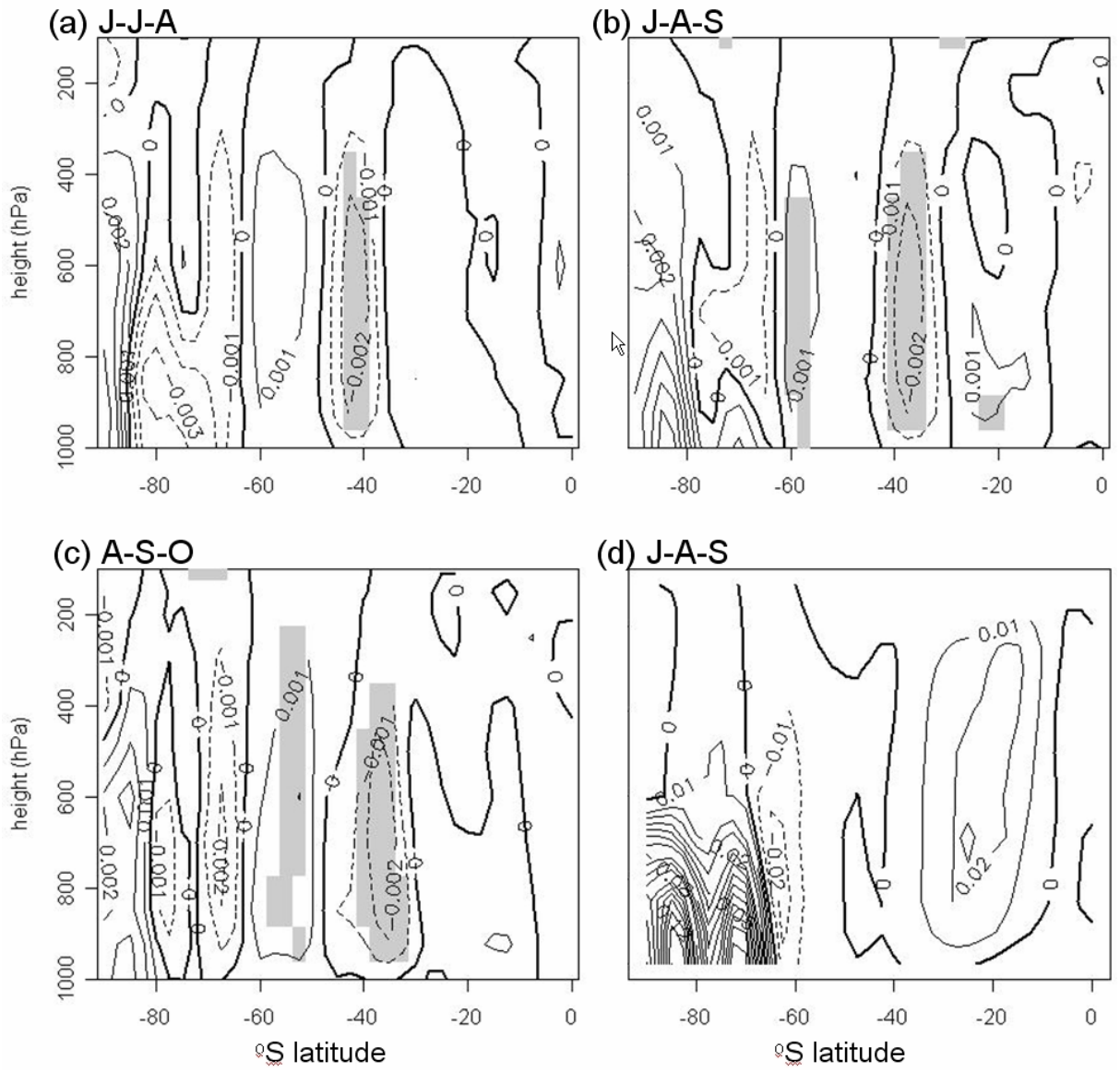

Figure 13. The zonally averaged vertical motion (omega $x10^{-2}$ hPa/s) difference between years of anomalously low-latitude ObsL and anomalously high-latitude ObsL for (a) June-July-August (b)July-August-Sept, (c) August-Sept-October. The mean for July-Aug-Sept is in (d). The solid line/positive values indicate downward motion, and the dotted lines/negative values indicate upward motion.

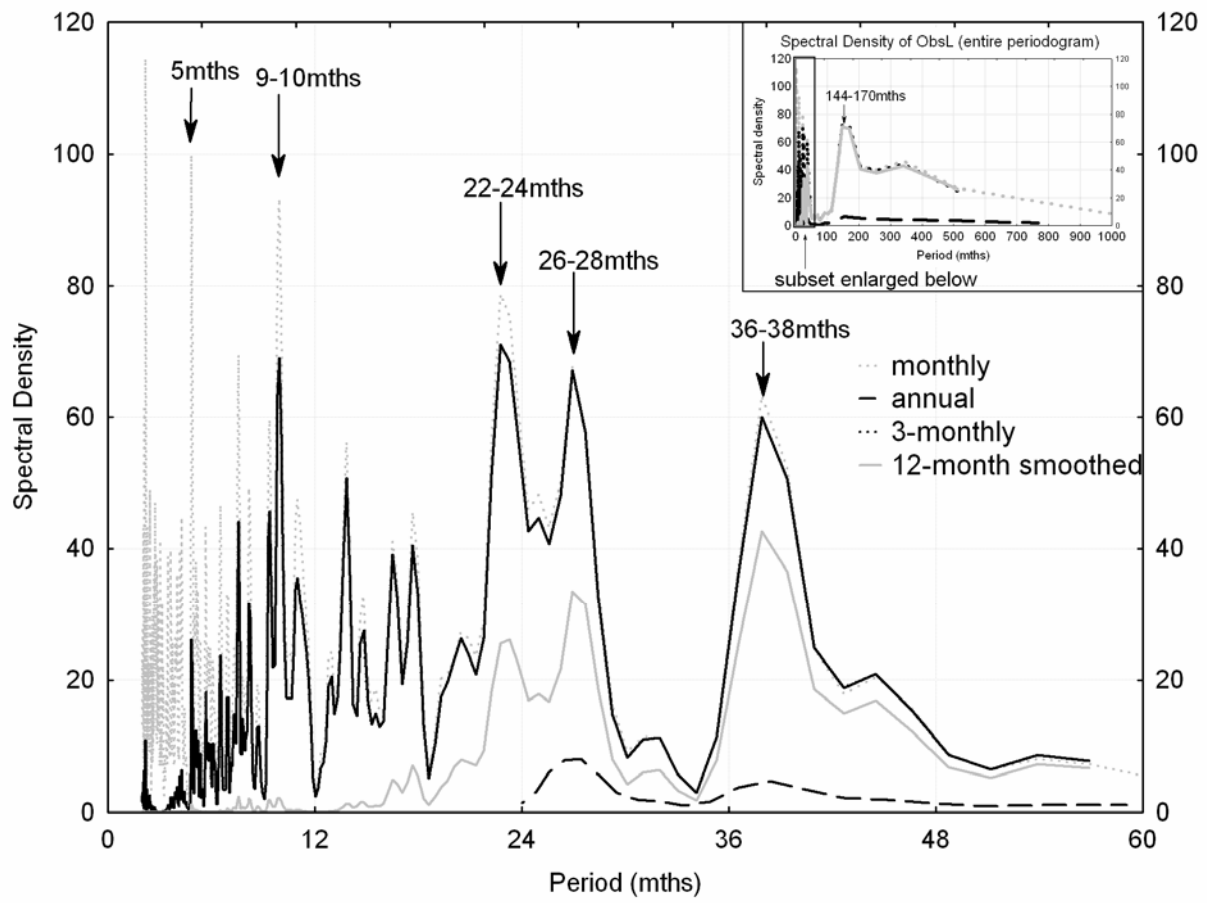

Figure 14. Spectral analysis of ObsL from 1959-2002. The raw data (monthly) are plotted as well three additional smoothed datasets: a January-December mean, a 3-month running mean, and a 12-month running mean. All data were detrended, tapered (15%), and padded. Hamming weights were used for the spectral densities. The entire periodogram is shown in the insert, and as the smaller periodicities are cluttered, those less than 60 months are shown in the main graph. The arrows indicate those cycles that are pronounced in all four datasets.

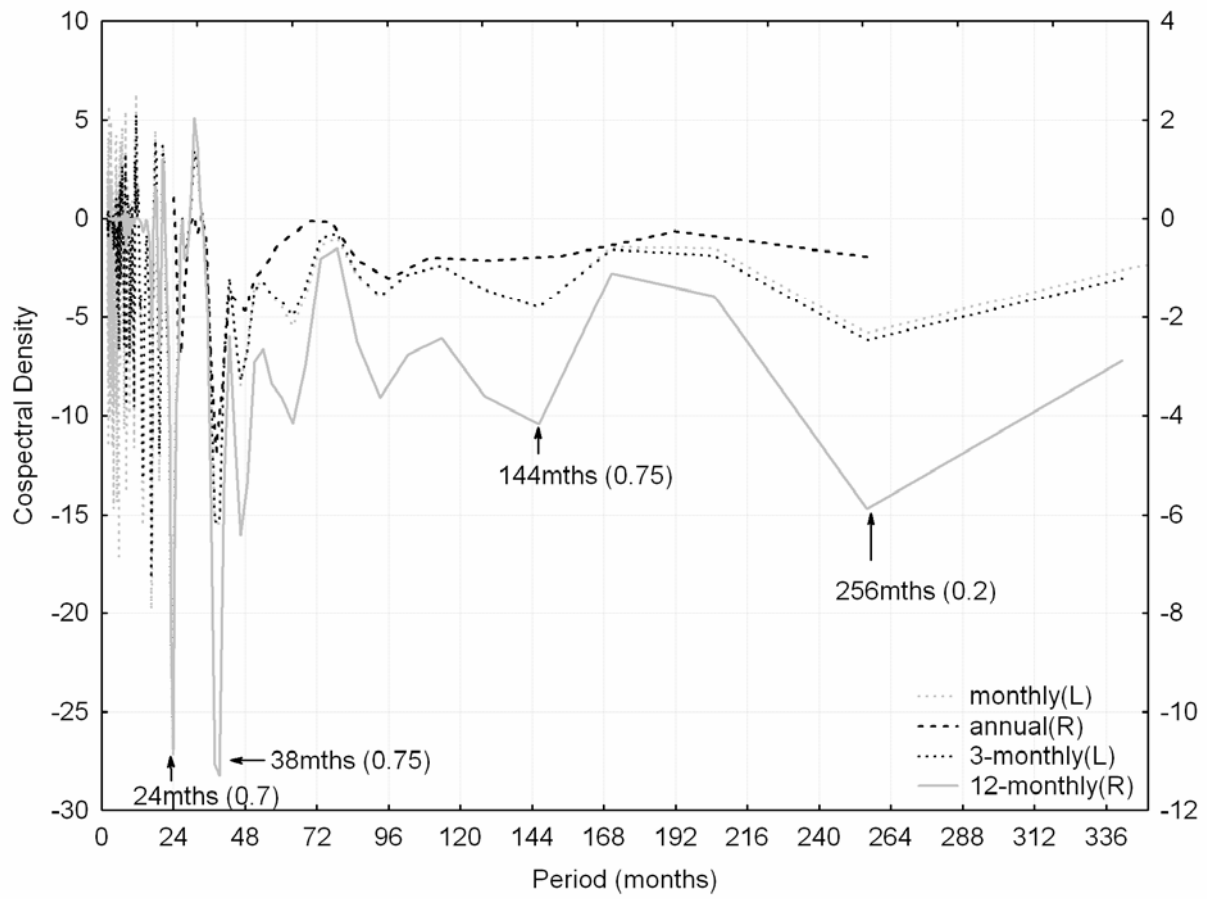

Figure 15. Co-spectral analysis of ObsL (dependant variable) and AOI-Marshall (independent variable). As per Figure 5, four different degrees of smoothing were applied to both time-series: "raw" monthly data, 3-month running mean, 12-month running means, and January-December mean. The values in brackets are the squared coherency values for those selected periodicities. The monthly and 3-monthly time-series are plotted against the left y-axis, and the annual and 12-monthly time-series are plotted against the right y-axis.

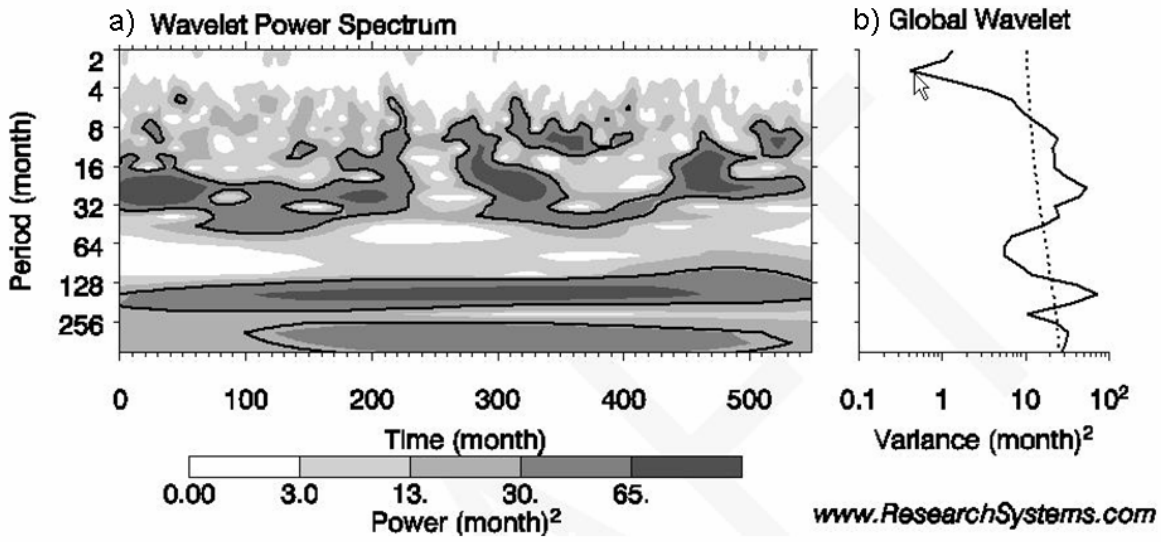

Figure 16. (a) The wavelet power spectrum of 3-monthly smoothed values of ObsL as per Torrence and Compo (1998) . The contour levels are chosen so that 75%, 50%, 25%, and 5% of the wavelet power is above each level, respectively. Black contour is the 5% significance level, using a white-noise background spectrum. (b) The global wavelet power spectrum (black line). The dashed line is the significance for the global wavelet spectrum, assuming the same significance level and background spectrum as in (a). Figure generated using software at

Table 1. Correlations and Trends of the different L indices. The data for the monthly correlations and trends have had the seasonal cycle removed. Note that the trend is the correlation coefficient between L and year (as per Drosdowsky 2005), not a regression coefficient. Italicized correlations are significant at the 0.05 level.

Correlations of annual L values. N=44. (correlations from a monthly time-series, n=516, are in brackets)

	HADL	OBSL	NCEPL	NCEPDL
HADL	1.00			
OBSL	***0.67 (0.62)***	1.00		
NCEPL	***0.53 (0.69)***	***0.60 (0.66)***	1.00	
NCEPDL	***0.64 (0.64)***	***0.74 (0.65)***	***0.78 (0.69)***	**1.00**

Trends of annual L values (trends using monthly values are in brackets)

	HADL	OBSL	NCEPL	NCEPDL
Over the period common to all datasets period 1959-2003. N=44 . (monthly N=516)	-0.01 p=.93 (-0.13 p=0.76)	0.17 p=.28 (0.05 p=0.21)	0.11 p=.46 (0.07 p=0.13)	0.16 p=.30 ***(0.09 p=0.04)***
Over the entire period of each dataset.	***-0.31 p=0.00 n=154*** ***(-0.11 p=0.00 n=1848)***	0.14 p=0.37 n=45 (0.05 p=0.29 n=540)	-0.013 p=0.93 n=55 (0.02 p=0.70 n=654)	0.12 p=0.38 n=55 (0.06 p=0.10 n=654)

Table 2. Pearson's correlation coefficient between monthly ObsL values, the SOI, and the AOI-Marshall. Values in **bold** are statistically significant at the 0.05 level.

	Jan	**Feb**	**Mar**	**Apr**	**May**	**Jun**	**July**	**Aug**	**Sept**	**Oct**	**Nov**	**Dec**	**All mths**
SOI	**-0.32**	-0.04	-0.06	-0.15	0.12	0.09	**0.33**	0.13	0.19	0.19	**-0.4**	**-0.29**	0
AOI	**-0.45**	-0.16	-0.06	**-0.32**	**-0.42**	**-0.29**	**-0.36**	**-0.44**	**-0.33**	-0.18	**-0.32**	-0.25	**-0.3**

Table 3. Pearson's correlation (r) and significance level (p) for 3-monthly averages of solar activity correlated with ObsL (top) and AOI-marshall (bottom). The most statistically significant values have been highlighted in bold italics.

		3-month seasons starting with month shown											
		1	**2**	**3**	**4**	**5**	**6**	**7**	**8**	**9**	**10**	**11**	**12**
ss vs L	**r**	0.01	0.04	-0.16	-0.15	-0.09	-0.01	0.19	0.24	0.23	0.15	0.05	0.07
	p	0.94	0.82	0.28	0.32	0.55	0.97	0.20	***0.12***	***0.12***	0.32	0.75	0.66
ss vs AOI	**r**	0.15	-0.01	-0.15	0.10	0.28	0.18	-0.08	-0.21	-0.13	-0.01	0.09	0.13
	p	0.34	0.95	0.32	0.52	***0.06***	0.24	0.60	***0.16***	0.37	0.95	0.58	0.41

Table 4. Relationships between 3-monthly averages of solar activity and the AOI-Marshall (top) and ObsL (bottom) when grouped according to QBO phase. Shown are Pearson's correlation coefficient (r), the p-value (p), and the range (diff) in degrees latitude of ObsL and the range of AOI-marshall values according to the respective linear regression equations where sunspots is the independent variable. The most statistically significant values have been highlighted in bold italics.

solar vs AOI		*3-month seasons starting with month shown*											
		1	**2**	**3**	**4**	**5**	**6**	**7**	**8**	**9**	**10**	**11**	**12**
QBO east phase	**r**	-0.13	***-0.40***	***-0.59***	-0.34	0.02	0.06	***0.47***	***0.41***	0.18	-0.16	-0.04	0.06
	p	0.60	***0.12***	***0.01***	0.20	0.95	0.85	***0.08***	***0.17***	0.55	0.55	0.88	0.84
	diff	-0.39	***-1.04***	***-1.43***	-0.78	0.00	0.13	***1.04***	***0.91***	0.39	-0.39	-0.13	0.26
QBO west phase	**r**	0.15	0.03	-0.05	0.13	0.22	0.17	***-0.27***	***-0.31***	***-0.30***	-0.16	0.00	0.09
	p	0.43	0.88	0.77	0.49	0.22	0.33	***0.13***	***0.07***	***0.08***	0.39	0.99	0.64
	diff	0.52	0.13	-0.13	0.39	0.65	0.52	***-0.78***	***-0.91***	***-0.78***	-0.52	0.00	0.26

solar vs L		*3-month seasons starting with month shown*											
		1	**2**	**3**	**4**	**5**	**6**	**7**	**8**	**9**	**10**	**11**	**12**
QBO east phase	**r**	0.03	0.11	-0.11	-0.10	-0.21	-0.09	-0.32	-0.26	-0.03	0.01	-0.07	-0.14
	p	0.90	0.70	0.69	0.73	0.47	0.78	0.26	0.39	0.91	0.96	0.79	0.62
	diff	0.13	0.52	-0.78	-0.52	-1.56	-0.65	-3.64	-2.34	-0.26	0.13	-0.65	-0.91
QBO west phase	**r**	0.00	0.01	-0.20	-0.18	-0.06	0.05	***0.45***	***0.39***	***0.33***	0.24	0.14	0.15
	p	0.98	0.98	0.30	0.33	0.74	0.78	***0.01***	***0.02***	***0.06***	0.21	0.48	0.44
	diff	0.00	0.00	-1.69	-1.82	-0.52	0.39	***3.51***	***3.51***	***3.25***	1.82	1.04	0.91